https://doi.org/10.5194/egusphere-2022-1133
Preprint. Discussion started: 10 November 2022

Excess methane, ethane, and propane production in Greenland ice core samples and a first isotopic characterization of excess methane

Michaela, Mühl[1], Jochen Schmitt[1], Barbara Seth[1], James E. Lee[2], Jon S. Edwards[3], Edward J. Brook[3], Thomas Blunier[4], Hubertus Fischer[1]

[1]Climate and Environmental Physics and Oeschger Centre for Climate Change Research, University of Bern, Bern, 3012, Switzerland
[2]Los Alamos National Laboratory, Earth Systems Observation, Los Alamos, NM 87545, USA
[3]College of Earth, Ocean, and Atmospheric Sciences, Oregon State University, Corvallis, OR 97331, USA
[4]Centre for Ice and Climate, Niels Bohr Institute, University of Copenhagen, Copenhagen, 2200, Denmark

Correspondence to: Michaela Mühl (michaela.muehl@unibe.ch)

Abstract. Air trapped in polar ice provides unique records of the past atmospheric composition ranging from key greenhouse gases such as methane (CH_4) to short-lived trace gases like ethane (C_2H_6) and propane (C_3H_8). Provided that the analyzed species concentrations and their isotopic fingerprints accurately reflect the past atmospheric composition, biogeochemical cycles can be reconstructed. Recently, the comparison of CH_4 records obtained using different extraction methods revealed disagreements in the CH_4 concentration for the last glacial in Greenland ice. Elevated methane levels were detected in dust-rich ice core sections measured discretely pointing to a process sensitive to the melt extraction technique. To shed light on the underlying mechanism, we performed targeted experiments and analyzed samples for methane and other short-chain alkanes ethane and propane covering the time interval from 12 to 42 kyears. Here, we report our findings of these elevated alkane concentrations occurring in dust-rich sections of Greenland ice cores. The alkane production happens during the melt extraction step (*in extractu*) of the classic wet extraction technique and reaches 14 to 91 ppb for CH_4 excess in dusty ice samples. We document for the first time a co-production of excess methane, ethane, and propane (excess alkanes) with the observed concentrations for ethane and propane exceeding their past atmospheric background at least by a factor of 10. Independent of the produced amounts, excess alkanes were produced in a fixed molar ratio of approximately 14:2:1, indicating a shared origin. The amount of excess alkanes scales linearly with the amount of mineral dust within the ice samples. The isotopic characterization of excess CH_4 reveals a relatively heavy carbon isotopic signature of (-46.4 ± 2.4) ‰ and a light deuterium isotopic signature of (-326 ± 57) ‰ in the samples analyzed. With the co-production ratios of excess alkanes and the isotopic composition of excess methane we established a fingerprint that allows us to confine potential formation processes. This fingerprint is not in line with a microbial

https://doi.org/10.5194/egusphere-2022-1133
Preprint. Discussion started: 10 November 2022

origin, rather such an alkane pattern is indicative of abiotic decomposition of organic matter as found in sediments, soils and plant leaves. This study provides first indications for an abiotic reaction producing excess alkanes during ice core analyses and discusses potential mechanisms.

We see an urgent need to correct the already existing discrete CH_4 records for excess CH_4 contribution ($CH_{4(xs)}$, $\delta^{13}C\text{-}CH_{4(xs)}$, $\delta D\text{-}CH_{4(xs)}$) in dust-rich intervals in Greenland ice. Specifically, excess CH_4 has a significant effect on the assessments of the hemispheric CH_4 source distribution. As we observe that in some intervals excess CH_4 is in the same range as the Inter-Polar Difference, previous interpretations of relative contribution of high latitude northern hemispheric CH_4 sources need to be revised.

1. Introduction

Atmospheric air entrapped in polar ice represents a unique archive of the past atmospheric composition including the concentration of greenhouse gases like carbon dioxide (CO_2) methane (CH_4) and nitrous oxide (N_2O) but also short-lived trace gases such as ethane (C_2H_6) and propane (C_3H_8). The ongoing anthropogenic increase in the atmospheric concentrations of these gases and the global warming caused by it makes a detailed understanding of their preindustrial variations and biogeochemical cycling of paramount importance and only polar ice cores are able to provide this information. However, to interpret reconstructions of the atmospheric composition from polar ice cores requires that archived atmospheric trace gases are not altered within the ice itself. Furthermore, the air must be extracted from the ice sample without altering the original composition. Thus, the comparison of ice core records obtained using different extraction techniques and from different ice cores requires careful consideration and interpretation.

It is known that not all drill sites or specific time intervals are equally suitable to derive pristine atmospheric trace gas records, for example CO_2 data from Greenland ice are subject to CO_2 in situ production due to impurities in the ice (Anklin et al., 1995; Smith et al., 1997). In situ production is also observed for N_2O, for example in glacial Antarctic ice core samples characterized by higher dust content (Schilt et al., 2010). In contrast, CH_4 in polar ice cores has been traditionally interpreted as "the good guy", which in the absence of melt layers is not affected by such processes. However, more recent results from Greenland showing elevated

https://doi.org/10.5194/egusphere-2022-1133
Preprint. Discussion started: 10 November 2022

CH_4 concentrations in glacial dusty ice (Lee et al., 2020) and high amplitude CH_4 spikes in Holocene ice (Rhodes et al., 2013, 2016) question this assumption.

This becomes especially worrisome as atmospheric methane also shows a North-South gradient reflecting the predominance of Northern Hemisphere sources. Bipolar ice core studies have been used to quantify this Inter-Polar Difference (IPD) in past CH_4 concentrations (Chappellaz et al., 1997; Baumgartner et al., 2012, Beck et al., 2018) with the goal to derive the contribution of northern and southern hemispheric sources to the overall CH_4 changes. The Holocene IPD is on the order of several tens of ppb, i.e., one order of magnitude smaller than the past atmospheric CH_4 concentration. Thus, any small CH_4 bias on the order of a few ppb has a strong impact on the conclusions drawn from this IPD, while the error on the total radiative forcing by such small biases is negligible. In summary, existing results of CH_4 concentrations from Greenland and Antarctic ice cores have to be carefully scrutinized for such effects.

A first step in this direction has been made in previous work by Lee et al. (2020), for example by comparing CH_4 records derived using different measurement techniques. Past CH_4 concentrations ($[CH_4]$) are retrieved by measurements of Greenland and Antarctic ice cores using traditional discrete and relatively new continuous melt extraction techniques. While discrete ice measurements deliver one single value for each sample, Continuous Flow Analyses (CFA) gradually melt a thin prismatic stick of the ice core providing a continuous record for this section. Although in both techniques the ice sample is melted, the CFA technique separates air from the melt water stream in about 1-2 min providing only a short time for any reaction in the water while for the discrete technique the contact time is typically 15-30 min.

Comparing $[CH_4]$ histories from several Greenland ice cores measured discretely (NGRIP, GISP2, GRIP) with the continuous Greenland NEEM and the continuous Antarctic WAIS record over the last glacial period, discrepancies in $[CH_4]$ between the existing records can be found in specific time intervals (Lee et al., 2020; Fig. 1 therein). These differences are particularly visible ~500 years prior to the onset of Dansgaard-Oeschger (DO) event 8 and 12 at around 39.5–40.0 kyears and 48.0–48.5 kyears, respectively, where the discrete NGRIP $[CH_4]$ record shows elevated values (~30 ppb) while the continuous NEEM and WAIS $[CH_4]$ records stay basically flat. Similar observations were also made on the GISP2 and GRIP record (Lee et al., 2020).

A closer look by Lee et al. (2020) into the existing records revealed further corollaries with other ice core parameters: intervals with elevated $[CH_4]$ in the discrete Greenland CH_4 record correspond to stadial ice with a high abundance of mineral dust (indicated by high Ca^{2+}

https://doi.org/10.5194/egusphere-2022-1133
Preprint. Discussion started: 10 November 2022

concentrations), especially visible again prior to DO-8 (and DO-12) when [CH_4] and [Ca^{2+}] simultaneously rise. When Ca^{2+} decreases again to low interstadial levels, [CH_4] drops by 10-20 ppb. Note that over the same intervals the corresponding continuous NEEM and WAIS CH_4 records remain stable.

Looking at the NGRIP methane hydrogen isotope (δD-CH_4) record (Bock et al., 2010b) – as well measured with a discrete melt-extraction technique (Bock et al., 2010a) – it turns out that in these anomalous sections, as explained above, the isotopic values are also affected. Several negative hydrogen isotopic excursions with a maximum depletion of 16 ‰ (permil) prior to the onset of DO-8 were identified (Bock et al., 2010b). At the time of that publication there was no straightforward explanation for these depletions (for example by a change in the source types) that could lead to "lighter" δD-CH_4 values during times of a relatively stable climate. Using ice from Antarctica much smaller δD-CH_4 variations during this interval were found (Iseli, 2019), again questioning the atmospheric origin of these δD-CH_4 depletions prior to the DO onset.

All these variations recorded in Greenland ice give reason to assume that a hitherto unknown process exists that produces or releases additional methane in some time intervals in Greenland ice cores (from here referred to as "excess methane" or $CH_{4(xs)}$). This process is related to the extraction technique (only found in records obtained by discrete melt extractions) and has only been observed in glacial Greenland ice with high mineral dust concentrations.

A first attempt to characterize $CH_{4(xs)}$ was made by Lee et al. (2020) who analyzed [CH_4] in discrete ice samples with different impurity composition and concentration from several ice cores (GISP2, NEEM, WAIS, SPICE) using a multiple melt-refreeze technique. With their data they were able to quantify $CH_{4(xs)}$ contributions of up to 30-40 ppb for Greenland samples. Sequential melt-refreeze extractions showed that the process leading to $CH_{4(xs)}$ is slow and not completed during the first cycle (i.e., within around 30 min). A special set of samples was analyzed with the admixture of a $HgCl_2$ solution to suppress microbial activity in the melt water. No difference in the measured [CH_4] was observed between the poisoned samples and replicates without $HgCl_2$. In addition, Lee et al., (2020) used the NGRIP [CH_4] (Baumgartner et al., 2014) and δD-CH_4 records (Bock et al., 2010b) to estimate the deuterium isotopic signature of the $CH_{4(xs)}$. Assuming a two-component mixture of atmospheric methane and excess methane their model led to a best estimate of (-293 ± 31) ‰ for δD- $CH_{4(xs)}$.

https://doi.org/10.5194/egusphere-2022-1133
Preprint. Discussion started: 10 November 2022

A straightforward explanation for $CH_{4(xs)}$ may be that CH_4 is either produced in the melt water, or it was produced beforehand and only released during the melt extraction. With respect to that, Lee et al. (2020) reviewed several mechanisms that could account for the observed variations in Greenland ice core records. None perfectly matched all their observations but lastly, three of the proposed mechanisms were short-listed: (1) an adsorption process on dust particles prior to the deposition on the ice sheet; (2) an in situ production in the ice; or (3) an abiotic reaction during melt extraction.

Here we resume the work by Lee et al. (2020) and shed more light upon the potential formation processes using a targeted and more comprehensive study to quantify $CH_{4(xs)}$. We analyzed specific NGRIP and GRIP ice core samples discretely with two different wet extraction systems. With our δ^{13}C-CH_4 device we are able to measure [methane], [ethane], [propane], and δ^{13}C-CH_4 on a single ice sample in two subsequent extractions. With our second device we add further data on δD-CH_4. In Sect. 2 we provide information on our sampling strategy and measurement techniques. With our new experimental results, presented in Sect. 3, we provide quantitative data for $CH_{4(xs)}$ in NGRIP and GRIP samples and extend our observations to other "excess alkanes" (ethane and propane), which are revealed to be co-produced during the excess CH_4 production. The observed molar ratios between methane, ethane, and propane are evaluated and their relation to the abundance of mineral dust (Ca^{2+}) within the ice samples is quantified. A 2nd extraction of the melt water enables us to estimate the temporal dynamics of excess alkane production. Using a Keeling-plot approach to our isotopic results, we calculate the carbon and deuterium isotopic signature of excess CH_4 (δ^{13}C-$CH_{4(xs)}$ and δD-$CH_{4(xs)}$). Based on our new and improved evidences, we finally come back to the discussion of the hypotheses by Lee et al. (2020) in Sect. 4 and offer potential mechanisms that could explain the excess alkanes in ice core samples.

2. Ice core samples and measurements

2.1 Ice core samples

Mixing ratios of alkanes (methane, ethane, and propane) and the stable carbon (δ^{13}C-CH_4) and hydrogen (δD-CH_4) isotope ratio of methane were measured on ice core samples from the North Greenland Ice Core Project (NGRIP) ice core. For this study, a total of 19 NGRIP ice core samples were measured for δ^{13}C-CH_4 and alkane concentrations and nine NGRIP ice samples

https://doi.org/10.5194/egusphere-2022-1133
Preprint. Discussion started: 10 November 2022

for δD-CH_4 covering the depth between 1795.84 m and 1933.25 m. The NGRIP samples stem from the late glacial Marine Isotope stages 3 and 2. These time intervals are characterized by sharp atmospheric CH_4 increases in parallel to rapid warmings, the so-called Dansgaard-Oeschger events, but we mostly sampled intervals with stable CH_4 concentrations.
From the same time period, we also investigate measurements of 41 NGRIP and 12 GRIP ice core samples which were carried out in 2011 and 2018, respectively, and which have not previously been published. See Fig. 1 for an overview of all analyzed NGRIP and GRIP ice core samples over time.

We also included 22 ice core samples from the European Project for Ice Coring in Antarctica (EPICA) ice core from Dome C that we use as long-term monitoring ice for the system performance and to quantify the blank contribution of the analytical system. Note that Antarctic ice core samples have not shown any signs of $CH_{4(xs)}$.
The late glacial time period, which includes the age of most of the measured NGRIP samples, is characterized by an overall high impurity and dust content and low atmospheric methane concentrations. For our analysis, we have selected ice core bags (where for NGRIP and GRIP ice cores, a bag is a 55 cm long ice core section) in which we expect the same atmospheric CH_4 concentration but a high range of mineral dust content (Ca^{2+}). In this way we can compare neighbouring samples that have the same low stadial CH_4 levels due to stable atmospheric concentrations and temporal smoothing by firn processes but are expected to vary in measured concentrations due to contributions of excess alkanes. Mineral dust content across our NGRIP samples range from 307 ng/g to 1311 ng/g.
This sample selection is also critical to quantify the isotopic signature of the $CH_{4(xs)}$ produced using the Keeling-plot approach (Keeling, 1958). The underlying assumptions of this mass balance approach are that (1) there is only a two-component mixture (atmospheric methane and excess methane) and that (2) the isotopic ratio of the mixture changes by a varying input of the second source ($CH_{4(xs)}$).

To select the samples, we use high-resolution mineral dust records measured using an Abakus laser attenuation device (Klotz, Germany) for particulate dust (Ruth et al., 2003) as well as Ca^{2+} concentrations derived from the Bern Continuous Flow Analysis System (Kaufmann et al., 2008) as dissolved mineral dust tracer (Erhardt et al., 2022). In principle, particulate dust and the specific soluble dust tracer Ca^{2+} are strongly correlated. However, dependent on acidity of

https://doi.org/10.5194/egusphere-2022-1133
Preprint. Discussion started: 10 November 2022

the ice (mainly due to H_2SO_4 and HNO_3), variable amounts of $CaCO_3$ are converted into soluble $CaSO_4$ and $Ca(NO_3)_2$ leading to a higher Ca^{2+}/ dust ratio (Legrand and Delmas, 1988).

As an example, Fig. 2 shows the Ca^{2+} and mineral dust concentration on the NGRIP depth of the NGRIP bag 3292 which we used to select the individual samples, and the relevant parameters measured for each sample of this bag. The data overview for all other measured NGRIP bags can be found in the Appendix A.

Note that all regression lines are calculated by following the method of York (1968) and York et al. (2004).

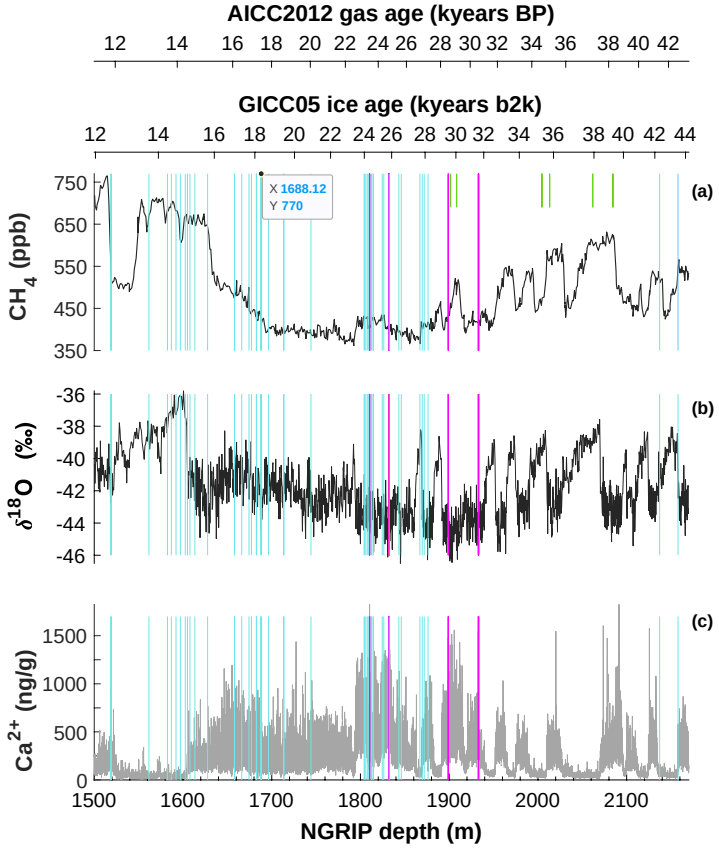

Figure 1: **Overview of the analyzed NGRIP and GRIP samples over time.** All analyzed NGRIP and GRIP ice core samples are indicated on the NGRIP depth (m) on the bottom axis and the AICC2012 gas age (kyears BP) & GICC05 ice age (kyears b2k) scale on the upper axes. NGRIP samples measured from the five main bags (3292, 3331 & 3332, 3453, 3515) for the Keeling-plot approach are indicated with vertical lines in pink, NGRIP samples measured in 2011 and individual NGRIP ice core samples measured in 2019-2020 (not included in the Keeling-plot analyses) in cyan, and GRIP ice core samples in green. **(a)** [CH_4] record measured from NGRIP samples from Baumgartner et al. (2012, 2014). **(b)** $\delta^{18}O$ record from North Greenland Ice Core Project members (2004). **(c)** Ca^{2+} record from Erhardt et al. (2022).

https://doi.org/10.5194/egusphere-2022-1133
Preprint. Discussion started: 10 November 2022

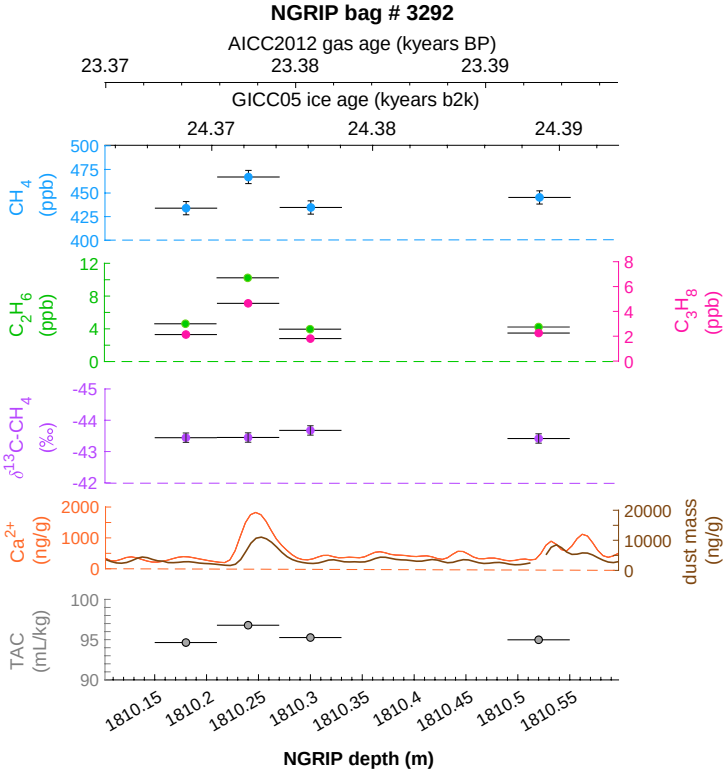

Figure 2: **Detailed data overview for NGRIP bag 3292.** Bag-specific overview of several parameters measured for each sample in this bag: methane, ethane, propane, Ca^{2+}, mineral dust mass, TAC (Total Air Content), $\delta^{13}C$-CH_4, indicated at the NGRIP depth (bottom axis) and the AICC2012 gas age (upper top axis) and the GICC05 ice age (lower top axis). The mineral dust record is taken from Ruth et al. (2003), the Ca^{2+} record from Erhardt et al. (2022). Here, this is shown exemplarily for the NGRIP bag 3292, the data overview for all further measured NGRIP bags can be found in the Appendix A.

https://doi.org/10.5194/egusphere-2022-1133
Preprint. Discussion started: 10 November 2022

2.2 CH_4, C_2H_6, C_3H_8 and $\delta^{13}C$-CH_4 Analysis of Ice Core Samples

The short-chain alkanes and $\delta^{13}C$-CH_4 were measured at the University of Bern using the discrete wet extraction technique as described in detail in Schmitt et al. (2014). With this method it is possible to measure mixing ratios of methane, ethane, and propane as well as the methane carbon isotopic signature and other trace gases on a single ice core sample of about 150 g.

Briefly, ice core samples are placed in a glass vessel locked by a stainless-steel flange which is attached to the vacuum line to evacuate laboratory air (see Fig. 3, step a). Before melting the ice sample, the leak tightness of the vacuum extraction line is tested with a so-called He blank. The ice sample is then melted under vacuum with the help of infrared radiation for ~35 min to release the enclosed air (step b). The released air is continuously removed from the sample vessel by a pressure gradient towards an adsorbing AirTrap (activated carbon), collecting all relevant air components at -180°C. After melting is completed, the temperature of the melt water is stabilized close to 0°C. Afterwards, He is flushed for ~14 min through a capillary at the bottom of the vessel to bubble He through the melt water to transfer any remnant gas species dissolved in the melt water onto the AirTrap (step c). The sample vessel is then sealed by closing inlet and outlet valves (step d). Consecutively, the AirTrap is warmed up in two steps to first remove N_2 and O_2 and in a second step to release the gases of interest which are then sent after a cryofocus step to the gas chromatograph (GC) for separation and quantification using an isotope ratio mass spectrometer (Isoprime 100, Elementar).

Precision of this method for CH_4 is about 5 ppb, 0.15 ‰ for $\delta^{13}C$-CH_4, and for both C_2H_6 and C_3H_8 the precision is 0.2 ppb or 5 % (whatever is higher) (Schmitt et al., 2014) for the typical NGRIP samples used in our study, where isotopic data are expressed using the δ notation on the international Vienna Pee Dee Belemnite (VPDB) scale. Blank levels for these species using this device are at 4 ppb for CH_4, 0.4 ppb for C_2H_6 and 0.3 ppb for C_3H_8.

With their experimental investigations, Lee et al. (2020) were already able to demonstrate that production/ release of $CH_{4(xs)}$ is time dependent. We therefore conclude that this process does not have to be completed in the time available for the gas extraction described above. We continued the analyses of excess alkane production with an additional extraction step (here referred to as 2nd extraction, steps d-g in Fig. 3) following the normal ice extraction routine. After all sample air is collected in the 1st extraction, the melt water is left in the sample vessel and held at temperatures close to 0°C for ~100 min (step d). After this "waiting time" of ~100

https://doi.org/10.5194/egusphere-2022-1133
Preprint. Discussion started: 10 November 2022

min, He is purged through the melt water for ~24 min to extract the gases that have been accumulated during this time interval (step f). The gases from this 2nd extraction are collected and measured following the same trapping and separation steps as in the 1st extraction. Note that the procedure of the 2nd extraction can be repeated any number of times (e.g. 3rd extraction).

The amount of gases that we obtain from the 1st extraction comprises the atmospheric amount, a possible contribution by in situ production, and a potential time-dependent production/release in the melt water (*in extractu*). The 2nd extraction, however, targets only the *in extractu* fraction. The system blank for the 2nd extraction was quantified using very clean Antarctic ice (Talos Dome, EDC) and is < 1% of the amount of extracted species in the ice extraction and lower than the measurement uncertainty.

Due to the small amount of CH_4 analyzed in this 2nd extraction (about a factor of 20 to 50 less than for an ice core sample) the precision for the $\delta^{13}C$ analysis is much lower than for the 1st (ice core) extraction and we estimate the precision of $\delta^{13}C\text{-}CH_4$ to 2 ‰ and for [CH_4] to be 2 ppb or 10 %. For C_2H_6 and C_3H_8, the precision is comparable to the 1st extraction. The blank values analyzed were 2 ppb, 0.3 ppb and 0.3 ppb for CH_4, C_2H_6 and C_3H_8, respectively, assuming an ice core sample air volume of 14 mL at standard temperature and pressure, which is the typical ice sample size of 150 g with a total air content of 0.09 mL/g.

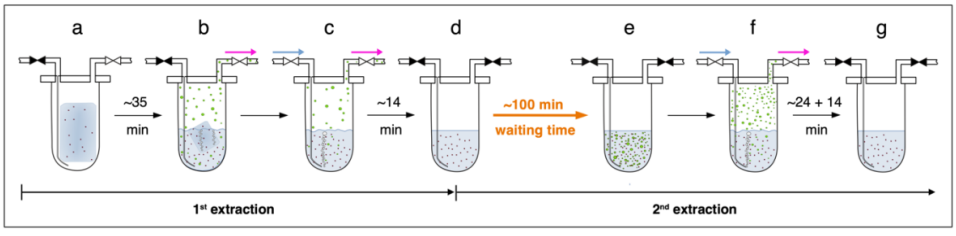

Figure 3: **Sequential steps (a-g) happening in the ice core sample vessel during the 1st and the 2nd extraction in the $\delta^{13}C\text{-}CH_4$ extraction line**. Scheme illustrates the subsequent steps as described in detail in the text. Brownish spots indicate dust particles in the ice/ melt water. Green circles indicate gas species (methane, ethane, and propane) in the melt water or in the headspace of the vessel. Closed valves are indicated in black, open vales in white. Blue arrows indicate the He flow through the inlet capillary into the sample vessel, pink arrows indicate the flow direction from the sample vessel towards the AirTrap.

https://doi.org/10.5194/egusphere-2022-1133
Preprint. Discussion started: 10 November 2022

2.3 δD-CH_4 Analysis of Ice Core Samples

All δD-CH_4 data presented here were measured at the University of Bern using the discrete wet extraction technique as described in detail in Bock et al. (2010a, 2014). This δD-CH_4 device allows to measure the concentration of methane and its deuterium isotopic signature (δD-CH_4).

Briefly, ice core samples are melted after evacuation of the headspace using a warm water bath at 40°C for 25-30 min to release the enclosed air into the sample vessel headspace. Once all the ice is melted, the warm water bath is replaced by an ice-water bath to keep the melt water temperature and water vapor pressure low. Note, in contrast to the δ^{13}C-CH_4 method, the inlet and outlet valves are closed during the melting process. The released air leads to an increased pressure in the sample vessel headspace enhancing the solubility of gases in water. Consecutively, the inlet and outlet valves are opened and He is purged for ~40 min with a flow of 360 mL/min to transfer the accumulated air in the headspace and bubble He through the melt water to strip dissolved gases. As for the δ^{13}C-CH_4 method, the air is collected on an activated carbon trap followed by further purification steps including GC separation. Note that compared to the δ^{13}C-CH_4 device, we performed only one extraction with the δD-CH_4 device.
For both methods, we assume that the time for an *in extractu* production during the ice extraction procedure starts with the first presence of melt water until He purging is stopped. Note that this time is considerably longer for the δD-CH_4 analysis (~90 min) compared to the time of the 1st extraction in the δ^{13}C-CH_4 analysis (~35 min).

Using this method we can measure [CH_4] and δD-CH_4 with a precision of about 15 ppb and 3 ‰ (based on standard ice sample measurements), where isotopic data are expressed using the δ notation on the international Standard Mean Ocean Water (SMOW) scale.

3. Characterization of excess alkanes in ice cores

3.1 Methane, ethane, propane concentrations

As described in detail in Sect. 2.2 a full ice sample measurement includes the regular ice sample extraction (1st extraction) and, after the waiting time of ~100 min, a 2nd gas extraction in the melt water. Gas from the 1st extraction is comprised of atmospheric air, a possible contribution from in situ production, a potential time-dependent contribution by an *in extractu* process, and

https://doi.org/10.5194/egusphere-2022-1133
Preprint. Discussion started: 10 November 2022

any contribution from the device itself (blank). For the gas species discussed here (methane, ethane, propane), these individual fractions are very different in magnitude. For polar ice core samples, the atmospheric air is the major fraction of methane even in dusty, glacial ice from Greenland prone to $CH_{4(xs)}$ production (see below). The opposite is true for ethane and propane, which are dominated by the *in extractu* component in dust-rich Greenland ice. To establish a better knowledge of alkanes in Greenland ice, we evaluated the measured concentrations of methane, ethane, and propane, their ratios to each other and the relation to the content of mineral dust in the ice with respect to the 1st and the 2nd extraction.

Note that different units to indicate concentrations of the trace gases of interest are used throughout this study. By using mixing ratios in units of [ppb], as typically used for atmospheric concentrations, the concentration of trace gases is related to the amount of air included in the ice. Ice core samples with a low air content cause higher mixing ratio values for any additional molecules produced in situ or *in extractu* compared to ice core samples with a high air content and the interpretation might be biased. Alternatively, for any additional molecules produced in situ or *in extractu*, [mol absolute per sample] denotes the absolute amount of trace gases and is independent of the ice core air content. In the following, both units are used and great care has to be taken to avoid misinterpretation of the results with respect to the different units.

3.1.1 Excess alkanes in the 1st extraction

Figure 4 and 5 show results from the 1st extraction of our NGRIP and GRIP ice core samples. For dust-rich samples, ethane ranges between 2 ppb and 12 ppb, and propane concentrations between 1 ppb and 5 ppb. In contrast, low-dust samples from both GRIP and NGRIP have much lower concentration (ca. 0.5 ppb for ethane, and 0.3 ppb for propane) consistent with estimates of past atmospheric ethane and propane concentrations from the 15th to 19th century of the common era being about 0.4 ppb over Greenland (Nicewonger at al., 2016) and lower for propane (Helmig et al., 2013). Emissions of ethane and propane were likely not drastically larger during the glacial (Bock et al., 2017; Nicewonger et al., 2016; Dyonisius et al., 2020) thus, 0.5 ppb appears to be an upper limit of past atmospheric concentrations of ethane and propane. This estimate of past atmospheric ethane concentrations is an order of magnitude smaller than the values we obtained from our dust-rich ice core samples from the 1st extraction, pointing to an additional source of these alkanes for dust-rich samples.

https://doi.org/10.5194/egusphere-2022-1133
Preprint. Discussion started: 10 November 2022

As illustrated in Fig. 5 (left panel), the ethane and propane concentrations are highly correlated, pointing to a common production of excess ethane and excess propane. The weighted mean ratio (weighted according to the number of samples measured per bag) and its weighted standard deviation (calculated by Gaussian error propagation of the weighted mean) is (2.25 ± 0.09) ppb ethane/ ppb propane. In Fig. 5, where the individual bags studied are color-coded, we can clearly see that the ratio is essentially the same between the individual bags and that the correlation is also very high within each bag (although we have to consider for the significance of this correlation that the number of samples per bag is very low). This indicates that for NGRIP ice ethane and propane are found in a fixed ratio. Accordingly, excess ethane and propane production can be well represented by the weighted mean ratio and ethane and propane are produced in a ratio of approximately 2:1. Very similar results were also observed in NGRIP samples measured in 2011 and in GRIP samples revealing an ethane to propane ratio of 2.14 ± 0.03 (r^2 = 0.99) and 2.00 ± 0.13 (r^2 = 0.99), respectively (see Fig. 5, left panel).
Note that for a coherent presentation throughout the paper and a better comparison, ethane is always plotted on the y-axis while we partly discuss ratios the other way round.

Methane concentrations range from 407 ppb to 476 ppb and are predominantly of atmospheric origin. The amount of $CH_{4(xs)}$ is the difference between the measured methane concentration and the atmospheric background concentration. To quantify $CH_{4(xs)}$ we use the fact that due to the low-pass filtering of the bubble enclosure process all samples within one bag should have the same atmospheric CH_4 concentration. This also ensures that any physical processes that potentially influence the atmospheric alkanes in our samples (gravitational enrichment, thermodiffusion, disequilibrium effects on CH_4 isotopes) are the same for all samples within one bag. The only difference between these samples is, thus, the degree of $CH_{4(xs)}$ production which is calculated from the linear fit between the measured CH_4 concentration and the concentration of another species (e.g. ethane, propane, mineral dust, or Ca^{2+}), which serves as a proxy for $CH_{4(xs)}$ production. The most precise relationship was found for [C_2H_6] and quantifying $CH_{4(xs)}$ was done by extrapolating the linear regression between ethane and methane to an ethane concentration of 0.39 ppb, the assumed atmospheric [C_2H_6]. This leads to an estimate of the true atmospheric [CH_4] value within the respective bag, a value that can then be subtracted from the measured CH_4 concentration to obtain the $CH_{4(xs)}$ in each sample. The uncertainty of the calculated $CH_{4(xs)}$ is typically 8 ppb. Using the relation of ethane to methane this approach translates into $CH_{4(xs)}$ in the range of 14 ppb to 91 ppb for these five NGRIP bags with a mean excess of 39 ppb. Note, this mean value is not representative for this time interval

https://doi.org/10.5194/egusphere-2022-1133
Preprint. Discussion started: 10 November 2022

as values are biased towards higher values as we intentionally selected samples with high Ca^{2+} content for our study. Equivalent calculations can be made using propane, dust, or Ca^{2+} as proxy for $CH_{4(xs)}$ production, however, the relationship between dust parameters and $CH_{4(xs)}$ is more variable and does not lead to equally precise values for $CH_{4(xs)}$. Nevertheless, the obtained mean $CH_{4(xs)}$ using the relation of mineral dust or Ca^{2+} to methane is similar to the one obtained by ethane.

We find that there is a constant production ratio between the measured excess alkanes. Production ratios are the average of single-bag ratios weighted by the numbers of samples measured per bag. Alkane concentrations were highly correlated within single-bags. The weighted mean ratio and its weighted standard deviation was calculated to be (6.42 ± 1.57) ppb methane / ppb ethane and (14.3 ± 3.7) ppb methane/ ppb propane for the samples of the five main NGRIP bags, and (2.25 ± 0.09) ppb ethane/ ppb propane (also including NGRIP2011 and GRIP here). We therefore characterize our measured NGRIP samples with an overall methane/ethane/propane ratio of approximately 14:2:1. This constant relationship between different alkanes suggests that excess alkanes are produced in a fixed ratio by a common production process.

Another important observation is the close relation between excess alkanes and the content of mineral dust within the ice core samples. Using measurements on GISP2 and NEEM ice core samples, Lee et al. (2020) reported for the first time the close relation of $CH_{4(xs)}$ to chemical impurities with the highest correlation with Ca^{2+}. This is supported by our measurements on NGRIP and GRIP samples revealing on overall increase of $CH_{4(xs)}$ as well as ethane and propane with increasing Ca^{2+} (Fig. 5, right panel). Although the connection between ethane and Ca^{2+} is more variable than for ethane and propane between the different bags, the slopes of the linear regressions in Fig. 5 (right panel) are still the same within the 2 σ uncertainty and the weighted mean ratio of all NGRIP samples amounts to (0.0089 ± 0.0024) ppb ethane/ (ng/g) Ca^{2+}.

However, this weighted mean value is likely biased low due to the relatively low ethane/ Ca^{2+} slope of bag 3515. Due to a data gap at 1932.7 m in the Ca^{2+} record, the corresponding Ca^{2+} concentration for two of the samples of this bag is subject to a large interpolation error and overestimated Ca^{2+} (see Fig. A3). Note also the mismatch in the peak shape of the Ca^{2+} and that of the dust mass suggesting an anomalous aerosol chemistry for this peak.

These results agree with results from GRIP and older NGRIP (2011) samples, revealing an ethane/ Ca^{2+} ratio of 0.0105 ± 0.0029 (r^2 = 0.76) and 0.0090 ± 0.0006 (r^2 = 0.91), respectively.

https://doi.org/10.5194/egusphere-2022-1133
Preprint. Discussion started: 10 November 2022

Based on the fixed ratio of excess CH_4 and ethane described above this translates into a weighted mean excess CH_4/Ca^{2+} ratio of (0.0529 ± 0.0111) ppb methane per (ng/g) Ca^{2+}. Note that due to the larger variability in the excess CH_4/ethane variation and the substantial variability in the ethane/Ca^{2+} relationship the relative uncertainty of this excess CH_4/Ca^{2+} relationship is relatively large and dust and Ca^{2+} are less suitable proxies to estimate $CH_{4(xs)}$ compared to ethane or propane.

Taken these findings together, we see a constant relationship between excess methane, ethane, and propane, but also a close relation to the content of mineral dust within the ice core sample, which, however, is not as tight as for the alkanes and suggests that dust parameters are only an indirect proxy of the alkane excess.

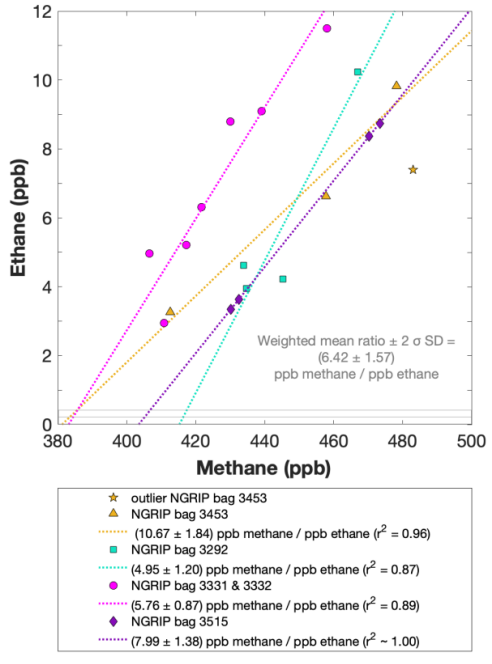

Figure 4: **NGRIP results of methane and ethane from the 1st extraction**. Concentrations of methane (ppb) and ethane (ppb) and their ratios to each other for NGRIP samples measured in the 1st extraction of the $\delta^{13}C$-CH_4 device. Different colors and symbols indicate the different NGRIP bags used for our analysis. Note that there is an outlier for CH_4 in bag 3453 as indicated in a yellow asterix, which is not included in the ratio of bag 3453. The grey hatched area indicates past atmospheric ethane concentrations of maximum 0.39 ppb as estimated by Nicewonger et al. (2016).

https://doi.org/10.5194/egusphere-2022-1133
Preprint. Discussion started: 10 November 2022

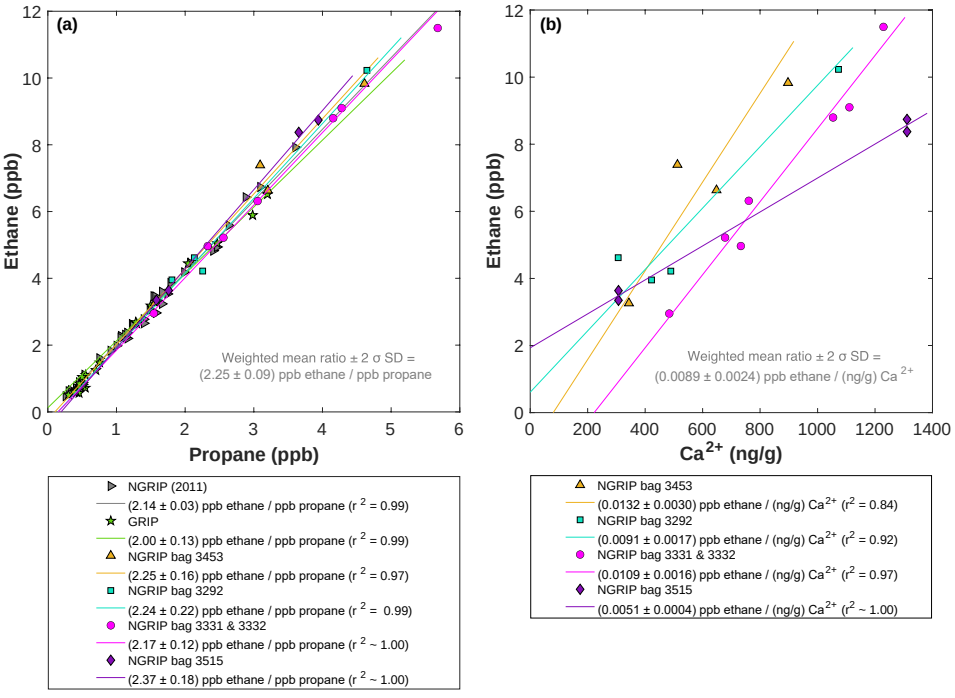

Figure 5: **NGRIP and GRIP results of ethane and propane from the 1st extraction. (a)** Concentrations of ethane and propane and their ratios to each other for NGRIP and GRIP samples measured in the 1st extraction of the δ^{13}C-CH_4 device. Colors and symbols indicate the different NGRIP bags or cores used. **(b)** Bag-specific production ratios of ethane in relation to the Ca^{2+} concentration for NGRIP samples. Note that for bag 3515 there is a data gap and an anomaly of the Ca^{2+} to dust mass ratio for the replicate sample at 1932.7 m and the Ca^{2+} concentration for these two data points is likely overestimated by a few 100 ng/g (see Fig. A3). Thus, the ethane/ Ca^{2+} slope for this bag is likely biased toward too high values.

3.1.2 Excess alkanes in the 2nd extraction

With the 2nd extraction in the δ^{13}C-CH_4 analyses we can evaluate the temporal dynamics of excess alkane production, assuming that gas extraction during the 1st extraction was quantitative and all alkanes extracted in the 2nd extraction were produced in the time after the 1st extraction was completed.

For our Greenland samples we measured a range of about 0.2 to 2.4 pmol for ethane and a range of 0.1 to 1.2 pmol for propane in the 2nd extraction. These values in pmol are equivalent to 0.2 to 48 ppb ethane and 0.2 to 2 ppb propane assuming that the amount of excess alkanes was added to 14 mL of ice core air (which is the typical ice sample size of 150 g with a total air content of 0.09 mL/g) (Fig. 6, right panel). The measured amount of methane ranges between

https://doi.org/10.5194/egusphere-2022-1133
Preprint. Discussion started: 10 November 2022

3 pmol and 20 pmol (Fig. 6, left panel). The ratio of the measured amount for the individual species between the 1st and the 2nd extraction amounts to 3.6 ± 0.85 (r^2 = 0.78) for ethane (Fig. 7, right panel), 3.3 ± 0.33 (r^2 = 0.78) for propane (combined data of NGRIP and GRIP) and 3.8 ± 1.62 (r^2 = 0.33) for methane (only NGRIP data), where the uncertainty for CH_4 is again much larger.

Thus, we can conclude that the amount of alkanes produced during the waiting time after the 1st extraction until the 2nd extraction was finished, was approximately 30% of the amount produced during the 1st extraction.

We can therefore safely conclude that excess alkanes are also produced/ released during the 2nd extraction. Results from the 2nd extraction also demonstrate that this process is slow and not completed during the time of the 1st extraction. We can thereby confirm the results of Lee et al. (2020) and here we are able to show for the first time that this process leads also to production of excess ethane and propane.

For a better estimate of the temporal reaction kinetics of the underlying process, we can relate the measured amount of the individual species to the time available for a potential reaction in the melt water during each extraction. For the five GRIP samples that were measured with a 2nd and 3rd extraction (see Sec. 2.1 and 2.2 for details) we take the cumulative production amount (where the first data point is the produced amount in the 1st extraction, the second data point is the sum of the 1st and 2nd extraction, and the third data point is the sum of the 1st, 2nd, and 3rd extraction). Exemplarily shown for ethane (Fig. B1, Appendix B) we can see the assumed first-order reaction kinetics with an exponential accumulation of ethane over time (accompanied by an exponential decay of organic precursor substances) providing a good model for our measurements. With that, we can estimate the half-life time (τ) of the production to be approximately 30 min. Compared to continuous flow techniques, where the reaction time before the air is separated from the liquid water stream, is only 1-2 min, only 5-10 % of the *in extractu* production found in our 1st extraction can be expected.

The goodness of fit of the ratios of the measured concentrations between the 1st and the 2nd extraction is r^2 = 0.78 for both ethane and propane, indicating that the production/release in the 1st extraction in relation to the 2nd extraction is well correlated for both species (Fig. 7b). Thus, samples that produced higher excess alkanes during the 1st extraction also produced more excess alkanes in the 2nd extraction suggesting that the production is dependent on the amount of some reactant present in the samples from which excess alkanes are produced. Again, for

https://doi.org/10.5194/egusphere-2022-1133
Preprint. Discussion started: 10 November 2022

CH_4 this relationship is more variable which is likely related to the higher uncertainty in measuring CH_4 for the 2nd extraction.

The ratio of ethane to propane of all measured Greenland samples in the 2nd extraction is 2.00 ± 0.07 ($r^2 = 0.99$). The ratio of methane to ethane is 8.34 ± 1.07 ($r^2 = 0.93$). Accordingly, the overall relationship between methane, ethane, and propane in the 2nd extraction can be characterized by a ratio of approximately 16:2:1. Comparing the ratios of ethane/ propane and methane/ ethane between the 1st and the 2nd extraction, there is no significant difference within the 2 σ uncertainties from 2.25 ± 0.09 to 2.00 ± 0.07, and from 6.42 ± 1.57 to 8.34 ± 1.07. We can conclude that within the error limits, the ratios stayed the same suggesting that the same *in extractu* process is at play during both extractions.

In the 2nd extraction, we can again observe the relation between excess alkanes and the amount of mineral dust. Figure 7 (left panel) shows the correlation of ethane (fmol/g melt water) to Ca^{2+} (ng/g) in all measured NGRIP and GRIP samples in the 2nd extraction revealing a production of (0.0085 ± 0.0011) fmol/(g melt water) ethane per (ng/g) Ca^{2+} with $r^2 = 0.70$. For methane, we observe a production ratio of (0.0556 ± 0.01513) fmol/(g melt water) methane per (ng/g) Ca^{2+} with a correlation of $r^2 = 0.47$ (data not shown).

Overall, excess alkane concentrations are increasing with increasing Ca^{2+} concentrations, in both the 1st and the 2nd extraction. The alkane production/release, however, decreased in the 2nd extraction, suggesting the progressive exhaustion over time of some reactant necessary for the *in extractu* process. We propose that this reactant co-varies with Ca^{2+} and particulate dust and that Ca^{2+} concentrations are only a proxy for higher *in extractu* production.

https://doi.org/10.5194/egusphere-2022-1133
Preprint. Discussion started: 10 November 2022

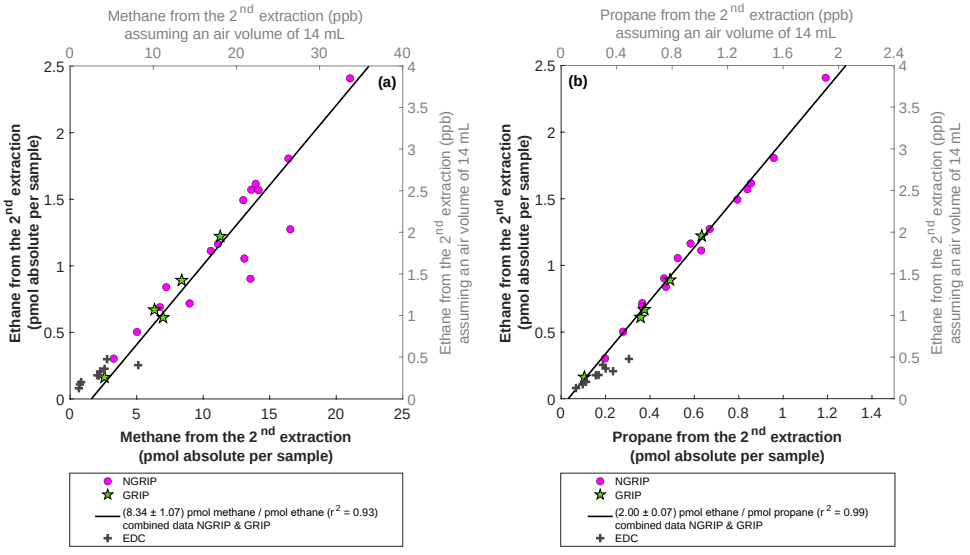

Figure 6: **NGRIP and GRIP results of excess methane, ethane, and propane from the 2nd extraction. (a)** Concentrations of methane and ethane and their ratios to each other. **(b)** Concentrations of propane and ethane and their ratios to each other. Units are given as pmol absolute per sample on the primary axis in black and in ppb assuming an air volume of 14 mL of the ice core sample on the secondary axis in grey. Grey crosses indicate the blank level of the system estimated from EDC ice core sample measurements.

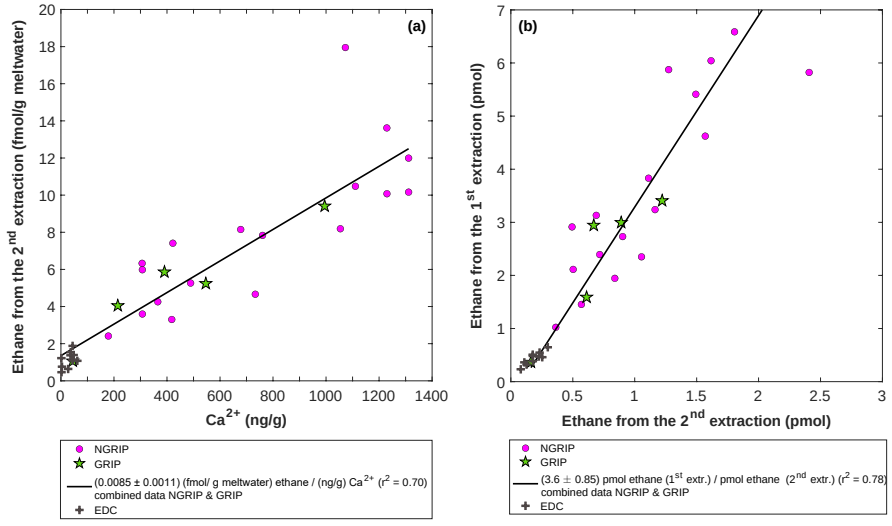

Figure 7: **NGRIP and GRIP results of ethane from the 2nd extraction in relation to the Ca^{2+} concentration and to the 1st extraction. (a)** Produced amount of ethane in the meltwater in relation to the Ca^{2+} concentration within the ice core samples. Grey crosses indicate the blank level of the system estimated from EDC ice core sample measurements. **(b)** Relation of the amount of ethane measured in the 1st and 2nd extraction.

https://doi.org/10.5194/egusphere-2022-1133
Preprint. Discussion started: 10 November 2022

3.2 Isotopic composition of excess methane

The evaluation of the carbon and deuterium isotopic signature of excess methane (δ^{13}C-$CH_{4(xs)}$ and δD-$CH_{4(xs)}$) is based on the Keeling-plot approach (Keeling, 1958, 1961; Köhler et al., 2006). Here, we want to characterize the isotopic signature of excess methane and explore how we can use this parameter to better identify its source or production pathway.

3.2.1 δ^{13}C-CH_4 isotopic signature of excess methane

Figure 8 (left panel) shows the δ^{13}C-CH_4 results of the 1st extraction. The carbon isotopic signature of excess CH_4 from the 1st extraction of the ice core sample measurements within one NGRIP bag are obtained from the y-intercept of the Keeling-plot, representing the excess δ^{13}C-CH_4 value for this bag. All bags show agreement in δ^{13}C-CH_4 signature (y-intercepts) within the 2 σ uncertainties. The weighted mean isotopic signature is (-46.4 ± 2.4) ‰, with weights assigned by the number of samples that constrained each individual Keeling plot regression line.

Figure 8 (right panel) shows the isotopic results in relation to the amount of CH_4 produced during the 2nd extraction. No atmospheric CH_4 is present during the 2nd extraction and the individual isotopic values in Fig. 8 (right panel) are the directly measured values of excess CH_4 without applying the Keeling-plot approach. For a better comparison, the produced CH_4 is shown both in pmol (lower axis in Fig. 8, right panel) and in a mixing ratio CH_4 scale (ppb), where we assume that the excess CH_4 produced during the 2nd extraction is diluted into an air volume of 14 mL at standard temperature and pressure, which is a typical value for the amount of air extracted from our samples in the 1st extraction.
The Keeling y-intercept values of the 1st extraction are added in the right panel of Fig. 8.

The δ^{13}C-CH_4 values of the 2nd extraction range between -34 ‰ and -48 ‰ with the mean being (-41.2 ± 2.2) ‰. This value is isotopically heavier compared to the weighted mean of (-46.4 ± 2.4) ‰ inferred from the Keeling analysis, however, is within the 2 σ error limits. We note that the measured peak areas for the 2nd extractions are very small and lie outside of the typical range of our gas chromatography mass spectrometry analysis for δ^{13}C-CH_4 and we cannot exclude some bias in these results. However, we mimicked these small peak areas with injections of small amounts of standard air and observed no significant bias in the measured

https://doi.org/10.5194/egusphere-2022-1133
Preprint. Discussion started: 10 November 2022

δ^{13}C-CH_4 values given that the precision of such small peaks is around 2 ‰. Another caveat is the considerable blank contribution for CH_4 that we observe for the 2nd extraction. Since Antarctic ice cores do not show a sizable *in extractu* production (Fig. 7, grey crosses for EDC) we measured EDC samples with the same protocol as for our Greenland samples to provide an upper boundary of this blank. As can be seen in Fig. 8 (right panel) the amount of CH_4 measured for these EDC samples (grey crosses) is on average about 2 pmol (equivalent to about 2 ppb). For comparison, our ice samples from Greenland show a range of about 5 to 20 pmol, thus we have a considerable blank contribution. However, the δ^{13}C-CH_4 blank signature obtained from these EDC samples is comparable to or only a few ‰ heavier than the δ^{13}C-CH_4 signature of the excess CH_4 from this 2nd extraction for the Greenland samples. Considering these analytical limitations of our 2nd extraction for δ^{13}C-CH_4, these findings suggest that excess CH_4 produced during the 1st and 2nd extraction has a similar δ^{13}C-CH_4 isotopic signature and is likely produced/released by the same process in both extractions.

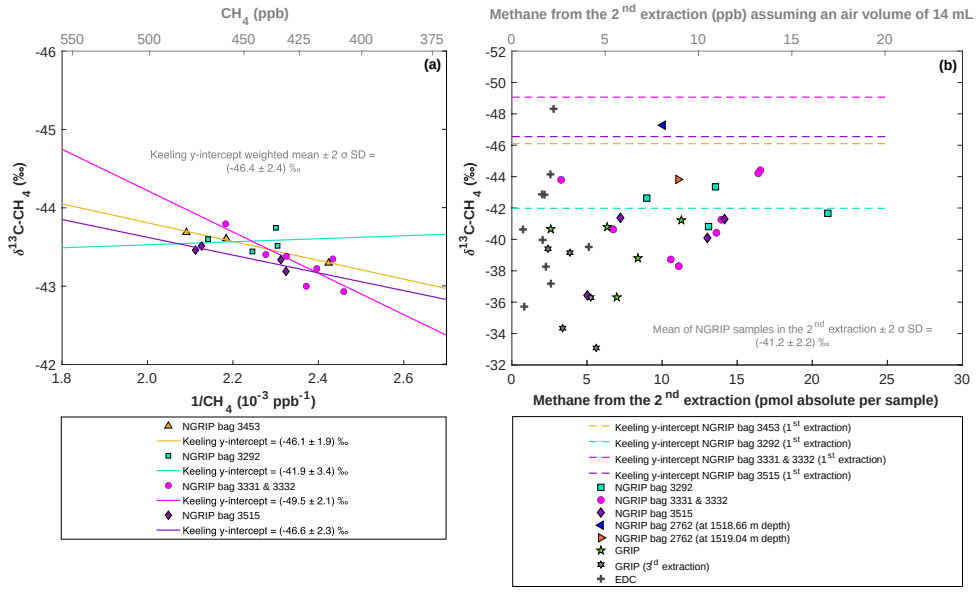

Figure 8: **NGRIP (and GRIP) δ^{13}C-CH_4 results of the 1st and 2nd extraction measured with the δ^{13}C-CH_4 device. (a)** Keeling-plot of δ^{13}C-CH_4 for NGRIP samples from the five main bags (3292, 3331 & 3332, 3453, 3515) measured in the 1st extraction. Colors and symbols indicate individual measurements of the respective bags. Colored lines indicate the corresponding Keeling regression line of each individual bag. **(b)** δ^{13}C-CH_4 (‰) values in relation to the amount of methane measured in the 2nd extraction. Units for CH_4 are given as pmol absolute per sample on the primary axis in black, and in ppb assuming an air volume of 14mL of an ice core sample on the secondary axis in grey. Colors and symbols indicate individual measurements of the respective bags. Color-coded lines indicate the corresponding Keeling y-intercept of each individual bag as measured in the 1st extraction. Grey crosses indicate the blank level estimated from EDC ice core measurements.

https://doi.org/10.5194/egusphere-2022-1133
Preprint. Discussion started: 10 November 2022

3.2.2 δD-CH_4 isotopic signature of excess methane

Figure 9 shows the isotopic results of the δD-CH_4 analyses. Due to the larger sample size required for the δD-CH_4 analyses and the sample availability restrictions only two bags were studied for δD-CH_4. The individual isotopic results obtained from the ice core sample measurements within one NGRIP bag are again combined into one Keeling y-intercept, representing the δD-CH_4 value for this bag. NGRIP bag 3460 (orange) reveals a Keeling y-intercept δD-CH_4 value of (-308 ± 51) ‰. The two NGRIP bags 3266 and 3267 (purple) are neighbouring bags and were therefore combined into one Keeling y-intercept revealing a δD-CH_4 value of (341 ± 62) ‰. The difference between the two Keeling y-intercepts of the individual bags is within the error limits and thus do not show significant differences. Accordingly, we combine the two values to a weighted mean and weighted uncertainty of (-326 ± 57) ‰.

Our results are consistent with the findings of Lee et al. (2020), who used the NGRIP δD-CH_4 record of Bock et al. (2010b) and the NGRIP [CH_4] record of Baumgartner at al. (2014) to estimate the δD-$CH_{4(xs)}$ signature in these samples. Assuming a two-component mixture of atmospheric methane and excess methane in their model led to a best estimate of (-293 ± 31) ‰ for δD-$CH_{4(xs)}$ which is within the error limits of our Keeling-plot results.

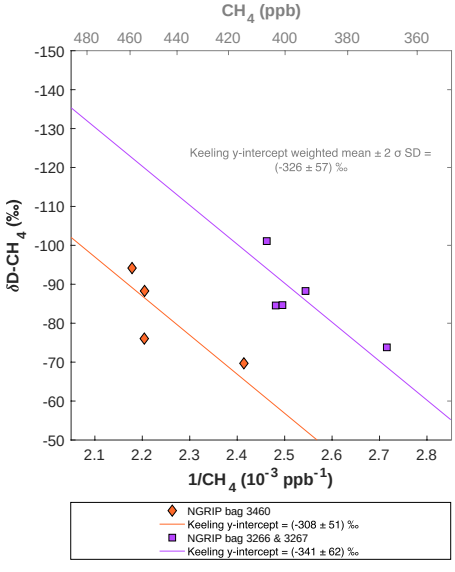

Figure 9: **GRIP δD-CH_4 results.** Keeling-plot of δD-CH_4 of NGRIP samples measured with the δD-CH_4 device. Colors and symbols indicate individual measurements of the respective bags and colored lines indicate the corresponding regression of each individual bag.

https://doi.org/10.5194/egusphere-2022-1133
Preprint. Discussion started: 10 November 2022

4. Testing the hypotheses explaining excess alkanes

In Sect. 3 several pieces of evidence for the production/release of excess alkanes in Greenland ice core samples were collected:

- We can confirm the observations of Lee et al. (2020) on excess methane in different Greenland ice cores and its covariance with the amount of mineral dust in the ice. Despite the different extraction techniques applied (multiple melt-refreeze method in Lee et al. (2020) versus two subsequent wet extractions in our study), we can further corroborate that the temporal dynamics of the production/ release is on the order of hours and production/ release occurs when liquid water is present during extraction.
- We document for the first time a co-production/ release of excess methane, ethane, and propane, with the observed values for ethane and propane exceeding by far their estimated past atmospheric background concentrations.
- Excess alkanes (methane, ethane, propane) are produced/ released in a fixed molar ratio of approximately 14:2:1, indicating a common origin.
- We further characterize the isotopic composition of excess CH_4 of $\delta^{13}C\text{-}CH_{4(xs)}$ and $\delta D\text{-}CH_{4(xs)}$ to be (-46.4 ± 2.4) ‰ and (-326 ± 57) ‰ in NGRIP ice core samples, respectively. Within error limits, our $\delta D\text{-}CH_{4(xs)}$ results are consistent with the calculated best estimate of (-293 ± 31) ‰ by Lee et al. (2020).

In the introduction we presented the hypotheses proposed by Lee et al. (2020) explaining their observations on $CH_{4(xs)}$. Here we resume the discussion of the original hypotheses and refine them in light of our new data from NGRIP and GRIP ice sample measurements. An overview of the different possible sources explaining excess alkanes is illustrated in Fig. 10. We believe that the origin of the observed excess alkanes falls in one of the three categories:

1.) Excess alkanes could be adsorbed on mineral dust particles prior to their deposition on the Greenland ice sheet and released in the laboratory during the prolonged melting process. The adsorption step could happen in the mineral dust source region (East Asian deserts) thereby adsorbing the alkanes from natural gas seeps within the sediment (process marked as A1, see Fig. 10). Alternatively, there is adsorption of atmospheric alkanes on dust particles either at the soil surface in the dust source region or during atmospheric transport to the Greenland ice sheet after deflation (A2). The desorption of the adsorbed alkanes happens during the melting process for both cases.

https://doi.org/10.5194/egusphere-2022-1133
Preprint. Discussion started: 10 November 2022

2.) Excess alkanes could be produced microbially. The production happens either in the ice itself (in situ) and the alkanes are then subsequently released during the melting phase in the laboratory (M1). Alternatively, the microbial production happens in the melt water during the melting process (*in extractu)* (M2). A microbial in situ production in the ice without an adsorption-desorption process was already ruled out by Lee et al. (2020) since it is not compatible with evidence from the CFA CH_4 concentration records. Excess CH_4 is not observed in CFA records implying that the extraction/production of excess alkanes is slow relative to the short extraction time of CFA. This was used as evidence for desorption of alkanes from mineral dust particles in the ice which would be released slowly at the presence of liquid water and effect techniques using longer extractions.

3.) Excess alkanes are produced abiotically, e.g. by the decomposition of labile organic compounds. This chemical reaction can happen either in the ice itself (in situ), which are then adsorbed on dust particles and subsequently released during the melting process (C1), or in the melt water during extraction (*in extractu*) (C2). An abiotic in situ production in the ice without an adsorption-desorption process can also be ruled out with the CFA evidence.

We now discuss these mechanisms in detail and evaluate the viability of the different hypotheses in the light of our new experimental observations.

https://doi.org/10.5194/egusphere-2022-1133
Preprint. Discussion started: 10 November 2022

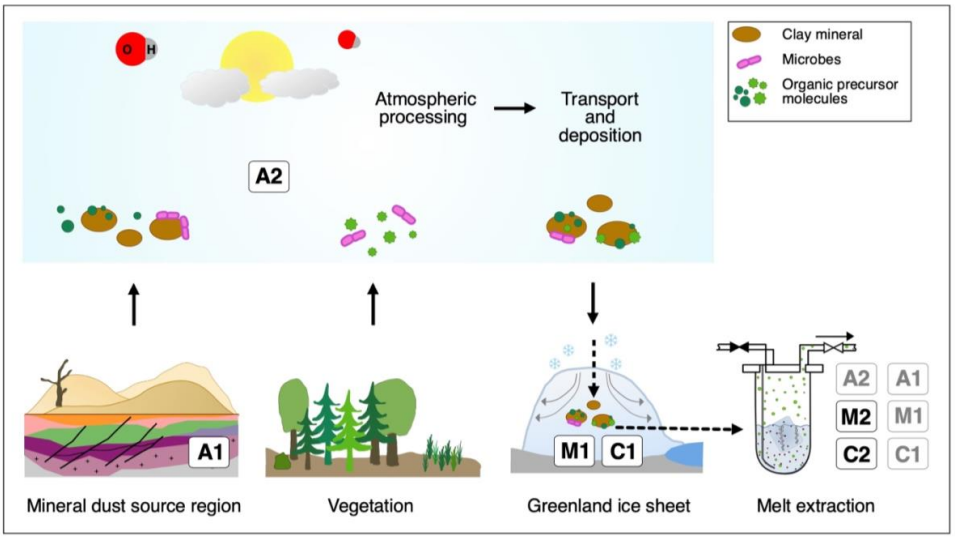

Figure 10: **Overview of the different possibilities explaining excess alkanes in dusty Greenland ice**. **A** depicts an adsorption process of alkanes on mineral particles, either from natural gas seeps within the sediment (A1) or from the atmosphere (A2) prior to their deposition on the Greenland ice sheet and in relation to a subsequent desorption process during the melting process in the laboratory. **M** depicts a microbial production of excess alkanes, either in the ice itself (in situ), and in relation to an adsorption process on dust particles after production in the ice and a subsequent desorption process during the melting process (M1), or in the melt water (*in extractu*) (M2). **C** depicts the abiotic/ chemical production of excess alkanes, either in the ice itself (in situ), and in relation to an adsorption process on dust particles after production in the ice and a subsequent desorption during the melting process (C1), or in the melt water (*in extractu*) (C2).

(1) Adsorption/release of alkanes on mineral dust particles

In the following section we discuss the mechanism to explain our observations which are based on the adsorption of excess alkanes onto mineral dust particles. Depending on where the adsorption takes place, the mineral particles might adsorb alkanes of different origin and composition. One possibility is that the adsorption already takes place within the sediment or soil of the dust source region, thus before deflation (A1). As proposed by Lee et al. (2020), the major source region of mineral dust arriving in Greenland during the glacial (Taklamakan, Tarim Basin) are also regions where natural gas seeps reach the surface (Etiope and Klusman, 2002; Etiope et al., 2008). Alternatively, the dust particles adsorb alkanes that are present in the atmosphere and the adsorption can either happen at the soil surface in the dust source region or en route to the Greenland ice sheet after deflation (A2). At first order, for the scenario A2 the fingerprint (isotopic composition and ratio of alkanes) of the adsorbed alkanes depends on the

https://doi.org/10.5194/egusphere-2022-1133
Preprint. Discussion started: 10 November 2022

734 past atmospheric composition but could be modulated by selective fractionation processes
735 during adsorption.
736
737 To be a viable mechanism for our problem, it requires that the adsorbed alkanes stay strongly
738 bound at the mineral dust particles while desorption is insufficient both during the atmospheric
739 transport and during the several hundred years the dust particle spends in the porous firn (age
740 of the firn at bubble close off). During the melting procedure the adsorbed alkanes would then
741 be released from their mineral dust carrier, which in case of Greenland during glacial times is
742 predominately consisting of clay minerals from the Taklamakan (and partly also Gobi) desert
743 (Bory, et al., 2003, Svensson et al., 2000; Ruth et al., 2003; Rhodes et al., 2013). However,
744 other additional dust sources exist with their relative contribution varying with climate
745 conditions (Han et al., 2018; Lupker et al., 2010).
746
747 Evidence on the adsorptive capacity of alkanes on clay minerals and its strong retention was
748 accumulating from several experimental studies (Sugimoto et al., 2003; Cheng and Huang,
749 2004; Dan et al., 2004; Pires et al., 2008; Ross and Bustin, 2009; Ji et al., 2012; Liu et al., 2013;
750 Tian et al., 2017). While all clay minerals are expected to be CH_4 adsorbents (Sugimoto et al.,
751 2003), this was predominantly demonstrated for kaolinite, chlorite, illite, and montmorillonite
752 (Sugimoto et al., 2003; Cheng and Huang, 2004; Ross and Bustin, 2009; Ji et al., 2012; Liu et
753 al., 2013; Tian et al., 2017). Influencing parameters for an adsorption-desorption process are
754 mainly pressure, temperature, clay mineral type, micropore size, surface area, organic carbon
755 content, and water/ moisture content (Sugimoto et al., 2003; Cheng and Huang, 2004; Dan et
756 al., 2004; Pires et al., 2008; Ross and Bustin, 2009; Ji et al., 2012; Liu et al., 2013; Tian et al.,
757 2017). Most interestingly for us, studies by Sugimoto et al. (2003) and Dan et al. (2004) on the
758 adsorption of CH_4 in micropores on the surface of clay minerals in dried and fresh lake sediment
759 showed that dried sediment still retains CH_4 and that dried and degassed sediment re-adsorbs
760 ambient CH_4 at standard pressure of CH_4 and room temperature. The amount of CH_4 adsorbed
761 in their samples is strongly dependent on pressure and temperature while increasing
762 temperatures and decreasing pressure lead to a stronger desorption. The addition of water/
763 moisture leads to a rapid desorption of already adsorbed gases (Sugimoto et al., 2003; Dan et
764 al., 2004; Pires et al., 2008; Ji et al., 2012; Liu et al., 2013).
765
766 These results in principle support our hypothesis of an adsorption-desorption process for our
767 glacial NGRIP and GRIP ice core samples, where alkanes (from fossil seeps or atmosphere)

https://doi.org/10.5194/egusphere-2022-1133
Preprint. Discussion started: 10 November 2022

would be adsorbed on dust particles and desorbed during the measurement procedure when liquid water is present. Independent of the origin of the alkanes (A1 or A2) the amount of alkanes deposited onto the Greenland ice sheet by this process would be diminished if mineral dust particles were already in contact with liquid water during the long-range transport which may lead to a loss of previously adsorbed alkanes already in the atmosphere.

Regarding our experimental results, the high correlation between mineral dust (Ca^{2+}) and excess alkanes observed in many Greenland ice cores would be generally in line with the theory of adsorption on mineral dust. In our data we see that the amount of released excess alkanes per Ca^{2+} is variable (especially in the 2nd extraction), which can be explained by a varying adsorption capacity of the mineral dust particles or a close relation between the adsorption capacity and the type of clay mineral (Sugimoto et al., 2003; Ji et al., 2012). However, to explain the constant ratio of methane, ethane, and propane of 14:2:1 in our samples with an adsorption mechanism, we need to discuss the potential origins of the adsorbed alkanes.

First, we find very high relative excess contributions of ethane and propane in our samples, while we see a small excess contribution for methane compared to the atmospheric background. If we assume a comparable adsorption for all three alkanes, this would imply a strong relative enrichment of ethane and propane over methane in the concentration of these gases during adsorption. This is not in line with the past atmospheric $CH_4/(C_2H_6+C_3H_8)$ ratio where past atmospheric ethane concentrations by Nicewonger et al. (2016) are an order of magnitude smaller (and propane concentrations even less) than the measured concentrations in our NGRIP and GRIP ice core samples. If we assume instead that excess alkanes have a thermogenic origin, we see that the ratio of methane, ethane, and propane for our samples of approximately 14:2:1, translated into a $CH_4/(C_2H_6+C_3H_8)$ ratio of ~5, is most consistent with a thermogenic origin, albeit more at the lower limit (see Fig. 11, left panel). However, we also have to question a selective adsorption capacity of mineral dust particles. If ethane and propane are preferentially adsorbed over methane, this would misrepresent the actual ratio between the three alkanes and falsify our interpretation of the origin.

To further evaluate the adsorption theory in the light of our experimental evidence, we now include the carbon and deuterium isotopic signature of $CH_{4(xs)}$ in our samples. In our NGRIP data we document a relatively heavy (enriched) δ^{13}C-$CH_{4(xs)}$ signature (in both extractions), which is close to the atmospheric value at that time but a light δD-$CH_{4(xs)}$ signature, which is close to the typical microbial signature (see Fig. 11 for an overview of isotopic signatures and

https://doi.org/10.5194/egusphere-2022-1133
Preprint. Discussion started: 10 November 2022

alkane ratios). In general, atmospheric values for δ^{13}C-CH_4 and δD-CH_4 are heavier in atmospheric CH_4 compared to the global CH_4 source mix due to the fractionation by atmospheric sink processes. Typical atmospheric values for the respective gas age of our measured Greenland samples derived from Southern Hemisphere ice core samples are in the range between -42 ‰ to -45 ‰ for δ^{13}C-CH_4 (Möller et al., 2013) and between -50 ‰ to -80 ‰ for δD-CH_4 (Möller et al., 2013; Bock et al., 2017; Dyonisius et al., 2020). Due to the geographic distribution of sources and sinks, the true Greenland values at the respective ages are a little lower. For example, the measured interhemispheric difference in δ^{13}C-CH_4 over the Holocene (Beck et al., 2018), when $CH_{4(xs)}$ is not observed, is less than 1 ‰ and given a reduction of Northern Hemisphere sources during the Glacial, -42 ‰ to -45 ‰ can be regarded as an upper limit for our glacial NGRIP samples. Thus, the EDML values provide a representative first-order estimate of atmospheric δ^{13}C-CH_4 also for our NGRIP ice core samples.

In comparison to the atmospheric source mix, microbially produced CH_4 is depleted in both heavy isotopologues ($^{13}CH_4$ and CH_3D) compared to the atmospheric value. Typical values for microbial CH_4 are in the range between -150 ‰ to -450 ‰ for δD-CH_4 (Whiticar, 1999) and between -55 ‰ to -70 ‰ for δ^{13}C-CH_4 (see also Fig. 11, right panel). Thermogenic emissions range between -25 ‰ to -55 ‰ for δ^{13}C-CH_4 (Etiope and Klusman, 2002;) and between -100 ‰ to -275 ‰ for δD-CH_4 (Whiticar, 1999; Etiope et al., 2007). Accordingly, while we expect that any adsorbed CH_4 of atmospheric origin would at first-order reflect the atmospheric δ^{13}C and δD signature of CH_4 and would not be able to strongly affect the isotopic composition of the CH_4 extracted from our ice core samples, CH_4 adsorbed at the dust source (e.g. thermogenic origin) would not be subject to the fractionation by atmospheric sinks and would have a strong leverage on the isotopic composition of extracted CH_4. For δD, where the atmospheric sink fractionation is very strong, any $CH_{4(xs)}$ can therefore lower the δD signature of the ice core sample drastically.

Our NGRIP samples reveal a δ^{13}C-$CH_{4(xs)}$ value (Keeling y-intercept weighted mean) of (-46.4 ± 2.4) ‰ which is within the error consistent with contemporaneous atmospheric values or with emissions from seeping reservoirs of natural gas. In contrast, our hydrogen isotopic measurements on NGRIP samples reveal a very light δD-$CH_{4(xs)}$ value (Keeling y-intercept weighted mean) of (-326 ± 57) ‰ similar to the estimates by Lee at al. (2020) and outside of the field of a thermogenic origin (see Fig. 11). While both the low $CH_4/(C_2H_6+C_3H_8)$ ratio and

https://doi.org/10.5194/egusphere-2022-1133
Preprint. Discussion started: 10 November 2022

the δ^{13}C-$CH_{4(xs)}$ could be indicative of a thermogenic source (A1), the light δD-$CH_{4(xs)}$ signature is far away from the atmospheric δD-CH_4 value and is also not in line with typical δD-CH_4 values of a thermogenic origin. Hence, our δD-$CH_{4(xs)}$ values render the adsorption scenarios A1 and A2 unrealistic candidates to explain our observations.

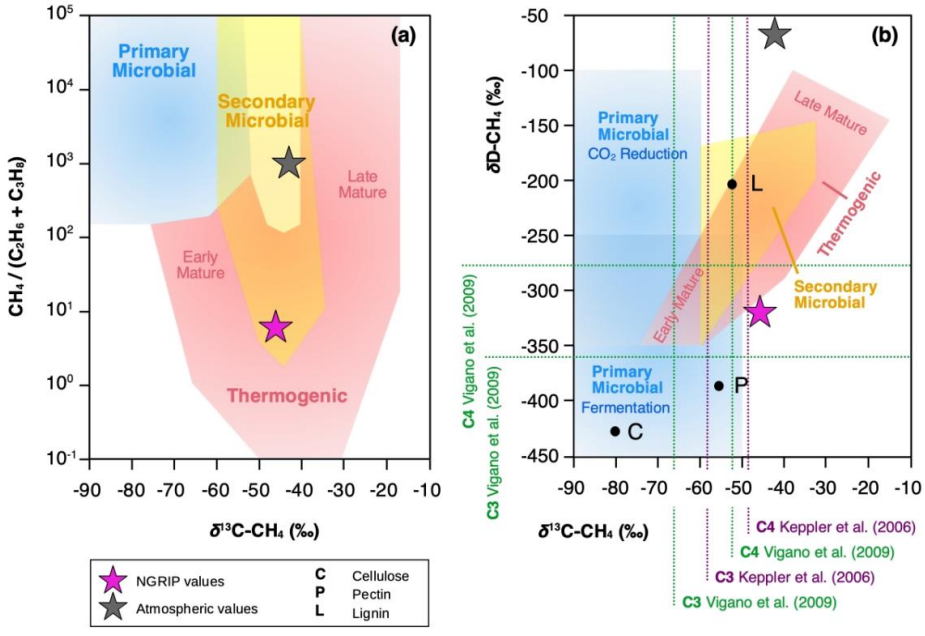

Figure 11: **Diagrams of genetic fields for natural gas adopted from Milkov and Etiope (2018). (a)** Genetic diagram of δ^{13}C-CH_4 versus $CH_4/(C_2H_6+C_3H_8)$. Typical atmospheric values are indicated with a grey star, NGRIP values obtained from this study with a pink star. **(b)** Methane genetic diagram of δ^{13}C-CH_4 versus δD-CH_4. Values for cellulose (C), lignin (L) and pectin (P) from Vigano et al. (2009) and mean values for C3 and C4 plants, respectively, from studies by Keppler et al. (2006) and Vigano et al. (2009) are added.

(2) Microbial production

The second process that we take into consideration regards the microbial production of excess alkanes through methanogenic microbes. Here we must again differentiate between two scenarios: a microbial production can either take place in the ice sheet itself (in situ) by extremophile microbes. This process requires that in situ produced excess alkanes are then adsorbed onto dust particles in the ice and subsequently desorbed during extraction when in

https://doi.org/10.5194/egusphere-2022-1133
Preprint. Discussion started: 10 November 2022

contact with liquid water (M1). Or the production takes place during the melt extraction when methanogenic microbes can metabolize in liquid water (*in extractu*; M2). Lee et al. (2020) already excluded a "simple" in situ production of excess CH_4 (microbial in situ production in the ice without an adsorption-desorption process) and this option will therefore not be further discussed here.

The viability of microbial in situ activity in the ice was substantially discussed in Lee et al. (2020) and references therein. While there is evidence for high cell counts in association with high concentrations of dust in Greenland ice cores, there is no direct evidence of active methanogens capable of producing CH_4 in ice (Tung et al., 2005, 2006; Rohde et al., 2008; Miteva et al., 2009). Calculations on the production of biogenic CH_4 in ice by Price and Sowers (2004), Tung et al. (2005), and Rohde et al. (2008) lead to a best estimate of ~$5 \cdot 10^{-5}$ pmol CH_4/g ice in 35 kyears. In comparison to our observations (for instance when taking the $CH_{4(xs)}$ mean of ~32 ppb in the four samples measured in the NGRIP bag 3515 with a mean ice sample weight of ~139 g) this translates into ~0.13 pmol CH_4/ g ice in 32 kyears, which is several magnitudes higher. Moreover, we assume that in situ produced excess alkanes would increase with time (depth) in relation to the amount of mineral dust within the ice until conditions no longer support this process (i.e. nutrient limitation). This was tested by analyzing dust-rich GISP2 samples ranging from 42-75 kyears, however, no time-dependent process was observed (Lee et al., 2020). On the other hand, there are CH_4 anomalies in Greenland ice cores that might be caused by microbial activity. Rhodes et al. (2013) report CH_4 spikes in the NEEM S1 core that are not associated with melt events but are characterized by anomalously high concentration of NH_4^+ and other biomass burning-derived nutrients. Since these CH_4 spikes have been observed both with the classic wet extraction and with the CFA technique that allows minimal reaction time in liquid water during the melt phase, these CH_4 anomalies were likely produced already in the ice, thus qualify as in situ. These narrow CH_4 spikes occur in Holocene ice with typically low dust and Ca^{2+} content, thus having a different impurity composition compared to our high-dust samples where we observe *in extractu* alkanes. Similar CH_4 spikes without an association to melt layers were reported in the GISP2 ice core by Mitchell et al. (2013).

Moreover, ice samples from different Greenland ice cores that are affected by melt events show CH_4 anomalies as well (Rhodes et al., 2016; NEEM Community Members, 2013). Further analyses are needed from these localized CH_4 spikes, e.g. if they show a co-production of ethane and propane as well and if their origin is really in situ or *in extractu* as well but with a much

https://doi.org/10.5194/egusphere-2022-1133
Preprint. Discussion started: 10 November 2022

quicker reaction time that allows the reaction to be completed within a few minutes (rather than hours in case of our *in extractu* phenomenon for dust-rich samples).

The second part of a potential M1 process, the adsorption of the microbially produced excess alkanes onto dust particles in the ice and the subsequent desorption during extraction, remains difficult to evaluate. In particular why should in situ produced alkanes be adsorbed onto mineral dust particles but not the atmospheric CH_4 that is anyway available in the air bubbles in the ice? Apart from these quantitative limitations of microbial CH_4 in situ production in ice, there is contradicting evidence from the "microbial inhibition experiment" by Lee et al. (2020) also for microbial production of alkanes during extraction. Lee et al. (2020) tested whether biological $CH_{4(xs)}$ production in the melt water was inhibited when the ice core samples were treated with $HgCl_2$. As $CH_{4(xs)}$ was still observed in the poisoned samples and as it seems quite unlikely that microbes are resistant to $HgCl_2$, this experiment questions the hypothesis of microbially produced $CH_{4(xs)}$ also during extraction (*in extractu*).

At this point, a microbial production process seems rather unlikely but is not definitively ruled out. However, our ratios of excess methane/ ethane/ propane in NGRIP and GRIP samples add another piece of corroborating evidence that excess alkanes are not produced microbially. The main microbial production process of methane, the decomposition of organic precursors in an anaerobic environment by archaea, also co-produces ethane and propane, however only in marginal amounts. The typical methanogenesis yields >200 times more methane than ethane and propane (Bernard et al., 1977; Milkov and Etiope, 2018) while we find a molar ratio of methane to ethane to propane of 14:2:1 in our samples. This renders a microbial production pathway (in situ and *in extractu*, i.e. M1 and M2) for excess alkanes unlikely. Moreover, a microbial production of CH_4 is unlikely in view of the $\delta^{13}C$-$CH_{4(xs)}$ signature which is too heavy for microbial CH_4.

We conclude that regardless of the production pathway, in situ or *in extractu*, the fingerprint of the produced excess alkanes in our samples (heavy $\delta^{13}C$-$CH_{4(xs)}$ signature and low $CH_4/(C_2H_6+C_3H_8)$ ratio) essentially rules out a microbial source and another (abiotic?) process for excess alkane production is likely to exist (see Fig. 11).

(3) Abiotic/ chemical production

In this last section we consider an abiotic or chemical process to be responsible for the observed excess alkanes, where excess alkanes would be produced through the abiotic decomposition of

https://doi.org/10.5194/egusphere-2022-1133
Preprint. Discussion started: 10 November 2022

labile organic compounds in the melt water (C2). Again, we disregard an abiotic in situ production in the ice (C1) based on the same arguments presented in the previous section for a microbial in situ production, as it would require the quantitative adsorption of the in situ produced alkanes onto mineral dust particles but not the atmospheric CH_4 that is available in the ice otherwise.

Organic precursors for this abiotic production during extraction could be any organic matter (either microbial or plant-derived). As the amount of excess alkanes is tightly coupled to the amount of dust, we assume that these organic compounds are attached to dust particles. This "docking" of the organic precursor onto the mineral dust could happen already in the dust source region involving organic material available at the surface (East Asian deserts). Or by adhering to volatile organic molecules or secondary organic aerosols from the atmosphere, either before deflation at the source region or during transport to Greenland. Note that organic substances might potentially experience abiotic preconditioning (ageing) during aerosol transport and only the final step of alkane production may occur during the wet extraction.

We consider this pathway, as in recent years the prevailing paradigm that methane is only produced by methanogenic archaea under strictly anaerobic conditions has been challenged. Several experimental studies demonstrated that methane can also be released from dried soils (Hurkuck et al., 2012; Jugold et al, 2012; Wang et al., 2013; Gu et al., 2016), fresh plant matter and dry leaf litter (Keppler et al., 2006; Vigano et al., 2008, 2009, 2010; Bruhn et al., 2009; Derendorp et al., 2010, 2011), different kinds of living eukaryotes (plants, animals and fungi) (Liu et al., 2015), single organic structural components (McLeod et al., 2008; Messenger et al., 2009; Althoff et al., 2014) and in fact under aerobic conditions. Most of these studies focused on methane, however, there is also evidence for simultaneous formation of other short-chain hydrocarbons like ethane and propane (McLeod et al. 2008; Derendorp et al., 2010, 2011). At least three mechanisms have been identified to be relevant: i) photo-degradation, ii) thermal degradation, or iii) degradation by the reaction with a reactive oxygen species (ROS) (Schade et al., 1999; Wang et al., 2017). Common to all three pathways is a functional group (for example a methyl or ethyl group) that is cleaved from the organic precursor molecule. Key parameters that control the production of abiotic methane are mainly temperature, UV radiation, water/ moisture, and the type of organic precursor material (Vigano et al., 2008; Derendorp et al., 2010, 2011; Hurkuck et al., 2012; Jugold et al., 2012; Wang et al., 2013, 2017). This "new" abiotic pathway of methane formation has not been discussed yet to be active during ice core

https://doi.org/10.5194/egusphere-2022-1133
Preprint. Discussion started: 10 November 2022

analyses, however, we believe that this process could be active during our melt extraction. In the following section we discuss the key parameters that generally influence abiotic production with respect to our measurement conditions and review the viability of this process for ice core samples and in the light of our experimental observations.

Recent findings demonstrated the large variety of potential organic precursors for abiotic trace gas formation. In general, the functional group cleaved from the precursor molecule defines the species to be produced, thus methyl- (or ethyl-) group containing substances for the production of methane (or ethane). For the formation of methane, the plant structural components pectin and lignin have been identified in many studies as a precursor in different plant materials. Pectin and lignin contain methoxyl-groups in two different chemical types, ester methoxyl (present in pectin) and ether methoxyl (present in lignin) (Keppler et al., 2006, 2008; McLeod et al., 2008; Messenger et al., 2009; Bruhn et al., 2009; Vigano et al., 2008; Hurkuck et al., 2012; Liu et al., 2015; Wang et al. 2017). Ester methyl groups of pectin were also discovered as precursor for ethane formation (McLeod et al., 2008). Overall, pectin makes up a large fraction of the primary cell wall mass of many plants, thus, representing a large reservoir available as organic precursor for abiotic alkane formation (Keppler et al., 2006; Mohnen et al., 2008; Vigano et al., 2008, 2010; McLeod et al., 2008), and may be present in sufficient quantities in our ice core samples attached to mineral dust particles. CH_4 production was also detected from cellulose even though it does not contain methoxyl groups suggesting that other carbon moieties of polysaccharides might allow abiotic CH_4 formation (Keppler et al., 2006; Vigano et al., 2008). In addition, poly-unsaturated fatty acids in plant membranes are suggested to play a key role not only in the formation of methane but also for ethane and propane (John and Curtis, 1977; Dumelin and Tappel, 1977; Derendorp et al., 2010, 2011). Further, sulfur-bound methyl groups of methionine are an important precursor for abiotic CH_4 formation in fungi (Althoff et al., 2014).

Considerably different emission rates were found for the same amount but different type of organic substances leading to the conclusion that abiotic emissions are strongly dependent on the type of organic precursor material or single structural components (Keppler et al., 2006; McLeod et al., 2008; Vigano et al., 2008; Messenger et al., 2009; Hurkuck et al., 2012). Other factors such as leaf and cell wall structure (McLeod and Newsham, 2007; Watanabe et al., 2012; Liu et al., 2015) and the organic carbon content (Hurkuck et al., 2012) are suggested to have an important influence on this process, too.

https://doi.org/10.5194/egusphere-2022-1133
Preprint. Discussion started: 10 November 2022

To explain the observed excess alkanes in dust-rich Greenland ice core samples by an abiotic production through the decomposition of labile organic compounds requires adequate quantities of organic precursors to be present within the ice core samples. Certainly, such material is present in Greenland ice, but currently, there is no record on the amount and type of organic substances in NGRIP and GRIP ice available. We have some limited information from occasional Greenland ice core samples in which different types of organic substances were detected (Giorio et al., 2018, and references therein), but it does not allow for an overarching interpretation for our ice samples. A NGRIP record on formaldehyde and a GRIP record on acetate and formate exists (Fuhrer et al., 1997), but as these substances are only representative for the respective dissolved organic compounds in the ice and not for any organic molecules attached onto the dust particles, they show lower levels during the glacial.

However, we also have to question whether a perfect record of eligible precursor molecules could at all exist. As we observe that precursor substances are labile and quickly decompose when in contact with liquid water, a direct measurement of these substances might not be possible but only for similar, non-reactive substances, which are then not qualified as precursors for the reaction observed. The problems of sampling, analysis and interpretation of organic material in polar ice are well summarized and expounded in Giorio et al. (2018).

In any case, it appears likely that the mineral dust, primarily coming from the Taklamakan and Gobi deserts (Biscaye et al., 1997; Bory et al., 2003), carries along soil organic matter or plant residues or accumulates organic aerosols as a result of organic aerosol aging during transport. In our data we see a relationship between the amount of mineral dust within the ice core samples and the amount of excess alkanes. As the amount of excess alkanes per Ca^{2+} (or mass of dust) is variable, this suggests that mineral dust is just a carrier for (a variable amount of) organic substances but does not account for the production of excess alkanes itself. The dust content within the ice core sample can therefore only serve as a rough estimate of organic precursor availability and whether an abiotic production from organic precursor substances is likely to occur during extraction.

Again, our experiments can shed some light on the viability of this pathway for excess alkane production. If we assume that the dust-related organic matter in the ice represents a reservoir available for an abiotic production, then the decomposition continues until all functional groups are cleaved from their organic precursor molecules and released as excess alkanes. Once the

https://doi.org/10.5194/egusphere-2022-1133
Preprint. Discussion started: 10 November 2022

reservoir is emptied excess alkane production ceases (Derendorp et al., 2010, 2011). In line, we interpret that the decrease in the amount of measured excess alkanes from the 1st to the 2nd extraction may result from an exhaustion of the precursor reservoir. The reaction time is slow enough to allow for the continuing production during the second extraction but too slow for a detectable production during continuous flow analysis of CH_4, where the water phase is present only for less than a minute before gas extraction. The significantly reduced production during the 2nd extraction in our samples shows that the time scale for this process is hours (see Fig. B1) until the reservoir of functional groups is depleted. We note that this implies that the amount of excess alkanes is strongly dependent on the time span when liquid water is in contact with the dust, which varies among the methods used for CH_4 analyses. Thus, any excess CH_4 in measurements from different labs performed under different conditions may differ.

To explain an abiotic alkane production, certain conducive boundary conditions must be met. The most important parameters that control non-microbial trace gas formation are temperature and UV radiation. This was demonstrated in many field and laboratory experiments (Keppler et al., 2006; McLeod et al., 2008; Vigano et al., 2008, 2009; Messenger et al., 2009; Bruhn et al., 2009; Derendorp et al., 2010, 2011; Hurkuck et al., 2012; Jugold et al., 2012; Wang et al., 2017). Generally, increasing temperatures lead to exponentially increasing CH_4 emissions (Vigano et al., 2008; Bruhn et al., 2009; Wang et al., 2013; Liu et al., 2015). The same behaviour was observed for ethane and propane with very low emissions at ambient temperatures (20-30°C) and a maximum at 70°C (McLeod et al., 2008; Derendorp et al., 2010, 2011). At constant temperatures emission rates decreased over time, which is at high temperatures on the timescale of hours and at ambient temperatures of months. Even after months, some production was observed, pointing to a slowly depleting reservoir of organic precursors (Derendorp et al., 2010, 2011). Increasing emissions observed at temperatures >40°C were also used as indicator to exclude the possibility of enzymatic activity, as the denaturation of enzymes would lead to rapidly declining emissions at higher temperatures (Keppler et al., 2006; Derendorp et al., 2011; Liu et al., 2015). We note that our sample extraction takes place at 0°C or a few °C above, hence, temperature conditions during the extraction are not conducive of the type of abiotic alkane production as observed in the studies listed above. Whether the cool temperature of the melt water during extraction inhibits abiotic reaction is difficult to conclude. Derendorp et al. (2010, 2011) observed a much lower temperature dependency of C2-C5 hydrocarbon emissions from ground leaves than whole leaves, which might also apply to our samples with very fine fragments of organic substances attached to dust particles.

https://doi.org/10.5194/egusphere-2022-1133
Preprint. Discussion started: 10 November 2022

Besides the strong relationship to temperature also UV irradiation seems to have a substantial effect on an abiotic production. Studies on irradiated samples (dry and fresh plant matter, plant structural components) showed a linear increase in methane emissions, while UV-B irradiation seems to have a much stronger effect on the release compared to UV-A (Vigano et al., 2008; McLeod et al., 2008; Bruhn et al. 2009; Jugold et al., 2012). The influence of visible light (400-700 nm), however, seems controversial (Keppler et al., 2006; Bruhn et al., 2009; Austin et al., 2016). Further, samples that were heated and irradiated show a different emission curve than just heated samples, indicating that irradiation changes the temperature dependency, in turn pointing to the fact that different chemical pathways exist (Vigano et al., 2008).
In dark experiments on plant material at different temperatures CH_4 emissions were still observed, while again higher temperatures revealed much higher emissions, emphasizing the strong temperature dependency also without UV irradiation (Vigano et al., 2008; Wang et al., 2008; Bruhn et al., 2009). The release of ethane along with methane from pectin was also stimulated under UV radiation (McLeod at al., 2008).

Regarding our measurements, the sample vessel in the δ^{13}C-CH_4 device is encased by a UV blocker foil absorbing the shortwave (<600 nm) emissions from the heating bulbs when melting the ice sample, while in the δD-CH_4 device the sample vessel is completely shielded from light (Sect. 2.2 and 2.3). Two NGRIP ice core samples were measured with the δ^{13}C-CH_4 device in the dark ("dark extraction") showing the same amount of excess alkanes as the regular measurements at day light. This indicates that light >600 nm has no influence on an *in extractu* reaction during our measurements. We stress that although we can exclude a direct UV effect during sample extraction, it is possible that UV irradiation during dust aerosol transport to Greenland and within the upper snow layer after deposition until the snow gets buried into deeper layers may precondition organic precursors attached to mineral dust to allow for alkane production to occur during extraction. In particular, the first step of the reaction (excitation of the homolytic bond of a precursor compound) may start already in the atmosphere or in the upper firn layer where energy from UV radiation is available. Within the ice sheet the reaction may be paused and only becomes reactivated during the melting process when liquid water is present.

Finally, we consider the role of reactive oxygen species in an abiotic production pathway. ROS are widely produced in metabolic pathways during biological activity but also during

https://doi.org/10.5194/egusphere-2022-1133
Preprint. Discussion started: 10 November 2022

photochemical reactions with mineral oxides (Apel and Hirt, 2004; Messenger et al., 2009; Georgiou et al., 2015). Through their high oxidative potential ROS are capable to cleave functional groups from precursor compounds. Several studies have demonstrated this mechanism for the production of abiotic CH_4 in soils and plant matter (McLeod et al., 2008; Messenger et al., 2009; Althoff et al., 2010, 2014; Jugold et al., 2012; Wang et al., 2011, 2013) and for other trace gases such as CO_2, ethane, and ethylene from plant pectins (McLeod et al., 2008). UV radiation or thermal energy has no direct influence on the degradation process by the reaction with ROS, however, it might also be a stimulating factor and evoke further indirect reactions. For instance, UV radiation can lead to changes in plants which in turn lead to ROS generation (Liu et al., 2015). It was demonstrated that UV radiation induces the formation of organic photosensitizers or photo-catalysts which increase CH_4 emissions from pectin (Messenger et al., 2009) and clay minerals. For example, the formation of OH from montmorillonite and other clay minerals upon UV (and visible light) irradiation shows that clays might play a significant role in the oxidation of organic compounds on their surface in different environments (Katagi, 1990; Wu et al., 2008; Kibanova et al., 2011).

It has been proven that the species type and the overall amount of ROS available for, or involved in a reaction, has a significant effect on the amount of emissions through such a process (Jugold et al., 2012; Wang et al., 2013, 2017). For the production of methane (and ethane), hydrogen peroxide (H_2O_2) and hydroxyl radicals (OH) have been proven to be the prominent species (Messenger et al., 2009; Althoff et al., 2010; Wang et al., 2011; Jugold et al., 2012; Wang et al., 2013, McLeod et al. 2008). Such ROS could be already present in the snow and ice or being produced in the melt water. For example, H_2O_2 can be unambiguously detected in Greenland Holocene ice using CFA, however, H_2O_2 in dusty glacial ice is mostly below the detection limit, likely due to oxidation reactions in the ice sheet or during melt extraction.

In summary, we believe that in our case of excess alkane production/ release in the melt water at low temperatures and without any UV irradiation the ROS-induced mechanism appears possible. In experiments with plant pectin McLeod et al. (2008) observed not only CH_4 but also ethane and found a methane to ethane production ratio of around 5 which is similar to our value of around 7. Accordingly, we see that a ROS-induced production pathway has the potential to explain excess alkanes in our samples, however, little is known about ROS chemistry in ice cores analyses in particular for reactions with organic precursors and more research is needed to understand the role of ROS in organic decomposition in ice.

https://doi.org/10.5194/egusphere-2022-1133
Preprint. Discussion started: 10 November 2022

Another key parameter influencing all abiotic pathways might be the presence of liquid water or moisture. In experiments testing the hypothesis of non-microbial CH_4 formation in different soil samples, it was demonstrated that the addition of water/ moisture led to an up to 8-fold increase in CH_4 emissions (Hurkuck et al., 2012; Jugold et al., 2012; Wang et al., 2013). It is hypothesized that the presence of liquid water or moisture stimulates (in addition to heating or UV radiation) the cleaving process of a functional group from the primary precursor compound and therefore increases the production of CH_4. However, it seems that the stimulating effect by water cannot be generalized, as Wang et al. (2013) emphasized that this process is highly dependent on "water of proper amount". In their experiments, CH_4 emissions from peat and grassland soil samples treated with a varying amount of water in oxia–anoxia cycles at 70°C were measured. They observed that under both aerobic and anaerobic conditions water does not always stimulate non-microbial CH_4 release and that too much water can also suppress CH_4 emissions. As Hurkuck et al. (2012) and Jugold et al. (2012) only observed a positive effect of water on CH_4 emissions in oxic soils, it is hypothesized that the amount of water they added to their samples is by chance in the stimulating range (Wang et al., 2013). In addition, Wang et al. (2013) observed differences between different soil samples in response to a varying water content indicating that the water effect is different for different precursors. With respect to our observations on NGRIP and GRIP samples the presence of water seems to be a fundamental parameter influencing an *in extractu* process, where the duration of water presence plays an important role in these reactions.

A final puzzle piece for a possible abiotic methane production comes from our dual isotopic fingerprints of the excess CH_4. As illustrated in Fig. 11 both $\delta^{13}C$ and δD of the CH_4 produced are in overall agreement with the carbon and hydrogen isotopic composition of potential organic precursors. For $\delta^{13}C$ our values lie on the heavier side of the isotopic carbon signature spectrum but still within the wide distribution of possible isotopic precursor signatures, for δD the signature lies well within the distribution.

We conclude that despite our inability to pinpoint the exact organic precursors that lead to abiotic excess alkane production during the melt extraction of our ice samples at this point, both the ratio of the excess alkanes as well as the isotopic signature of excess CH_4 is generally in line with this pathway. Thus, without further contradicting evidence from targeted studies on organic precursors in ice core samples and their degradation by ROS, we believe that the ROS-induced production pathway is the most likely explanation for the observed excess alkane production during extraction.

https://doi.org/10.5194/egusphere-2022-1133
Preprint. Discussion started: 10 November 2022

5. Conclusions and Outlook

The comparison of methane records from ice cores samples measured with different extraction techniques requires careful consideration and interpretation. Non-atmospheric methane contributions to the total methane concentration were discovered in specific Greenland ice core sections pointing to a process occurring during the wet extraction. To better assess this finding, we measured new records of [methane], [ethane], [propane], δD-CH_4, and δ^{13}C-CH_4 on discrete NGRIP and GRIP ice core samples using two different wet extraction systems. With our new data we confirm the production of $CH_{4(xs)}$ in the melt water and quantify its dual isotopic signature. With the simultaneous detection of ethane and propane we discovered that these short-chain alkanes are co-produced in a fixed ratio pointing to a common production pathway. With our 2nd extraction we constrained the temporal dynamics of this process, which occurs on the timescale of an hour.

Based on our new experimental data we provide an improved assessment of several potential mechanisms that could be relevant for the observed variations in NGRIP and GRIP ice samples. A microbial CH_4 production represents an obvious candidate but regardless of whether this CH_4 is produced in situ or *in extractu*, several lines of evidence gained from our measurements (low $CH_4/(C_2H_6+C_3H_8)$ ratio, heavy δ^{13}C-$CH_{4(xs)}$ signature) demonstrate that the fingerprint of the produced excess alkanes is unlikely to have a microbial source. Also an adsorption-desorption process of atmospheric or thermogenic CH_4 on dust particles does not match many of our observations (low $CH_4/(C_2H_6+C_3H_8)$ ratio, light δD-$CH_{4(xs)}$ signature) and is therefore unlikely. However, with the current knowledge we cannot definitely exclude such a process to be responsible for the observed excess alkane levels in our samples.

At present we favor to explain the formation of excess alkanes by abiotic decomposition of organic precursors during prolonged wet extraction. Such an abiotic source for methane and other short-chain alkanes was discovered previously in other studies (Keppler et al., 2006; Vigano et al., 2008, 2009, 2010; Messenger et al., 2009; Hurkuck et al., 2012; Wang et al., 2013, and others listed above) using different organic samples, e.g. from plant or soil material, however, this process has not been connected to excess CH_4 production in ice core analyses. This process matches many of our observations and such a mechanism can be responsible for excess alkanes in Greenland ice core samples. To better assess a potential abiotic production process in ice analyses the most important questions to solve in the future are: What are the specific precursor substances? Which parameters control an abiotic production during wet

https://doi.org/10.5194/egusphere-2022-1133
Preprint. Discussion started: 10 November 2022

extractions? How does the fixed molar ratio between methane, ethane, and propane come about in this process? And finally, in which way is this excess alkane production causally related to the amount of mineral dust within the ice sample?

Identifying a specific reaction pathway that leads to the short-chain alkanes with their observed ratios would certainly benefit from identifying targeted organic precursor substances in the ice. However, detecting these postulated organic precursors in the ice core is inherently difficult as these compounds must be very labile in water as our experiments demonstrated that after about 30 min only a fraction of these compounds remains in the melt water while the majority already reacted to excess alkanes. Future studies may also focus on further isotopic measurements (δ^{13}C-CH_4 and δD-CH_4) including isotope labeling experiments providing an option to unambiguously detect methane produced during the measurement procedure in a commonly used wet extraction technique, and again, to uncover potential reaction mechanisms for $CH_{4(xs)}$ production.

To better assess the viability of the alternative hypothesis of a release of previously adsorbed alkanes from dust particles (scenario A1 and A2) during the extraction, dust particles from the Taklamakan or Gobi desert need to be tested whether they contain relevant amounts of adsorbed alkanes that are released when in contact with liquid water. A second step could be to expose such dust samples to high levels of alkanes to mimic the adsorption process of natural gas seeps. It also needs to be shown that the adsorbed alkanes stay adsorbed on the dust particles for a prolonged time (months, ideally years) after exposing the particles to ambient air and that droplet and ice nucleation during aerosol transport does not lead to a loss of the previously adsorbed CH_4. To quantify any isotopic fractionation involved with the ad- and desorption step, δ^{13}C-CH_4 and δD-CH_4 analyses will be most valuable.

Finally, our studies clearly show that the published Greenland ice core CH_4 record is biased high for selected (glacial) time intervals and needs to be corrected for the excess CH_4 contribution. This is particularly important for studies of the IPD in CH_4 and stable isotope ratios of methane. Methodological ways to remedy excess methane (and ethane and propane) in future measurements of atmospheric [CH_4] from air trapped in ice cores could be to use continuous online CH_4 measurements, which apparently avoid $CH_{4(xs)}$ production. But also dry extraction methods and sublimation techniques for discrete samples, which are expected to avoid *in extractu* production by evading the melting phase, could be used. Finally, our own

https://doi.org/10.5194/egusphere-2022-1133
Preprint. Discussion started: 10 November 2022

δ^{13}C-CH_4 device, which allows to measure δ^{13}C-CH_4 as well as methane, ethane, and propane concentrations from the same sample, can be used to correct the measured CH_4 values making use of the co-production of the other two alkanes.

It is clear that $CH_{4(xs)}$ needs to be corrected for when interpreting the already existing discrete CH_4 records and its stable isotopes in dust-rich intervals in Greenland ice core samples. Impact of $CH_{4(xs)}$ on interpreting past atmospheric [CH_4] will only slightly affect radiative forcing reconstructions, however, it will have a significant effect on the assessment of the global CH_4 cycle and in particular on the hemispheric CH_4 source distribution which is based on the IPD. We observe that in some intervals $CH_{4(xs)}$ is in the same range as the previously reconstructed IPD implying that correcting for $CH_{4(xs)}$ will lower the IPD considerably and hence lower also the relative contribution of northern hemispheric sources at those times. We see that there is the urgent need to reliably revisit Greenland ice core CH_4 records for the excess CH_4 contribution and in future work we aim to establish an applicable correction for excess methane ($CH_{4(xs)}$, δ^{13}C-$CH_{4(xs)}$, δD-$CH_{4(xs)}$) in existing records using the co-production ratios of methane, ethane, and propane, the isotopic mass balance of excess and atmospheric CH_4 in ice core samples as well as the overall correlation of excess CH_4 with the mineral dust content in the ice.

https://doi.org/10.5194/egusphere-2022-1133
Preprint. Discussion started: 10 November 2022

Appendix A

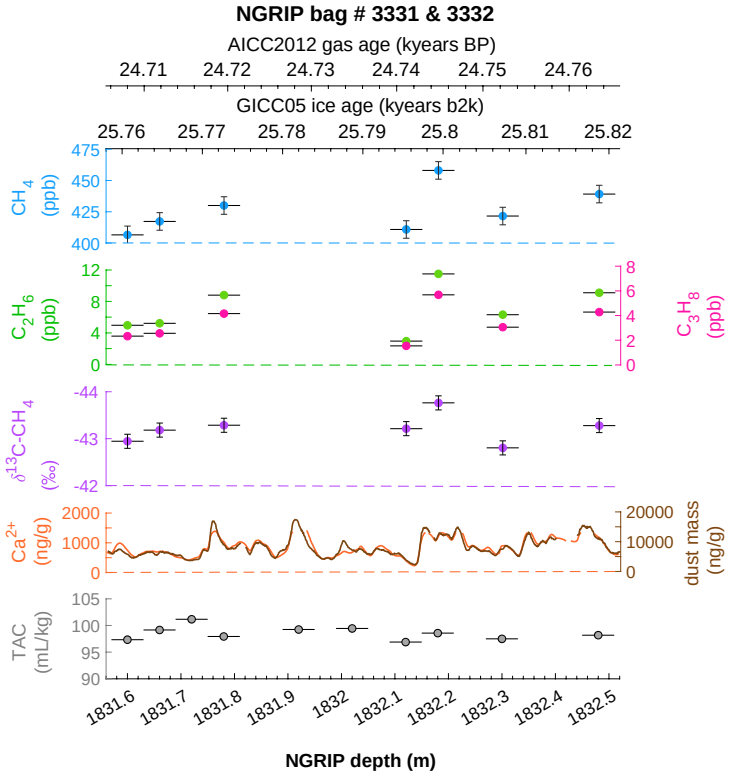

Figure A1: Detailed data overview for the neighbouring NGRIP bags 3331 & 3332. Bag-specific overview of several parameters measured for each sample in this bag: methane, ethane, propane, Ca^{2+}, mineral dust mass, TAC (Total Air Content), $\delta^{13}C\text{-}CH_4$, indicated at the NGRIP depth (bottom axis) and the AICC2012 gas age (upper top axis) and the GICC05 ice age (lower top axis). The mineral dust record is taken from Ruth et al. (2003), the Ca^{2+} record from Erhardt et al. (2022).

https://doi.org/10.5194/egusphere-2022-1133
Preprint. Discussion started: 10 November 2022

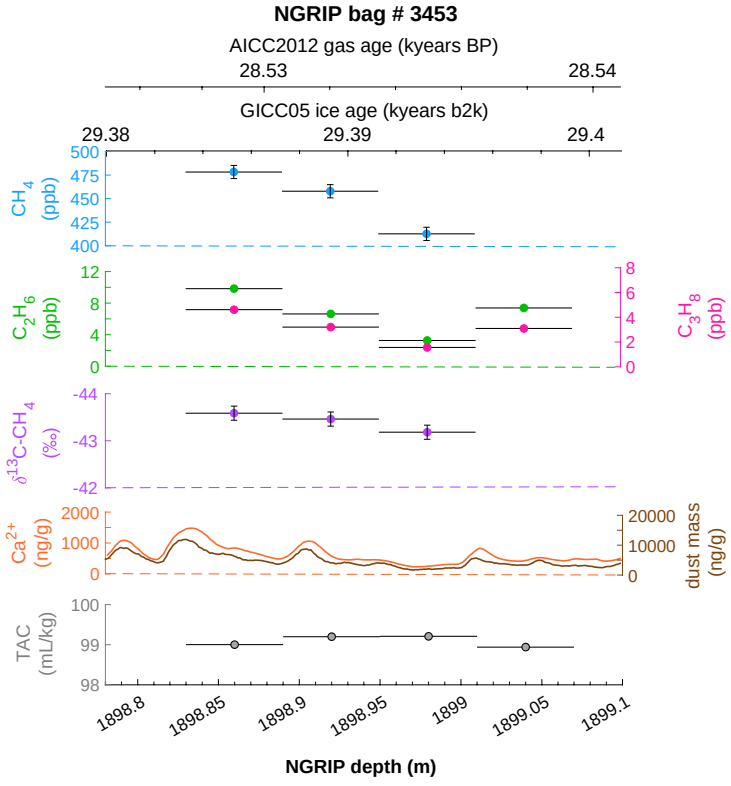

Figure A2: Detailed data overview for NGRIP bag 3453. Bag-specific overview of parameters measured for each sample in this bag: methane, ethane, propane, Ca^{2+}, mineral dust mass, TAC (Total Air Content), $\delta^{13}C\text{-}CH_4$, indicated at the NGRIP depth (bottom axis) and the AICC2012 gas age (upper top axis) and the GICC05 ice age (lower top axis). The mineral dust record is taken from Ruth et al. (2003), the Ca^{2+} record from Erhardt et al. (2022).

https://doi.org/10.5194/egusphere-2022-1133
Preprint. Discussion started: 10 November 2022

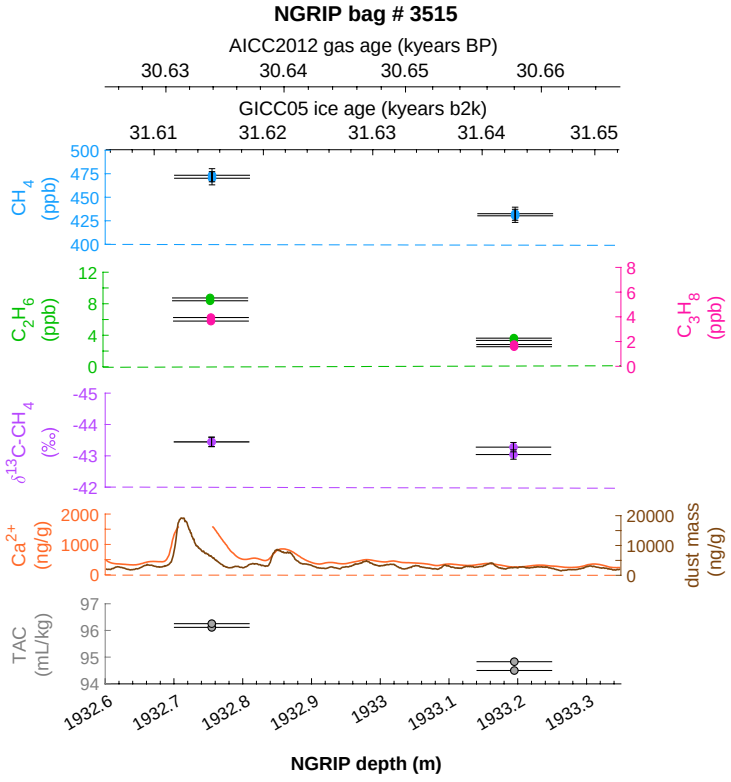

Figure A3: Detailed data overview for NGRIP bag 3515. Bag-specific overview of parameters measured for each sample in this bag: methane, ethane, propane, Ca^{2+}, mineral dust mass, TAC (Total Air Content), $\delta^{13}C\text{-}CH_4$, indicated at the NGRIP depth (bottom axis) and the AICC2012 gas age (upper top axis) and the GICC05 ice age (lower top axis). The mineral dust record is taken from Ruth et al. (2003), the Ca^{2+} record from Erhardt et al. (2022). Note that there is a gap in the Ca^{2+} record which was corrected by a fill routine for the analysis of the two measured samples at this depth.

https://doi.org/10.5194/egusphere-2022-1133
Preprint. Discussion started: 10 November 2022

Appendix B

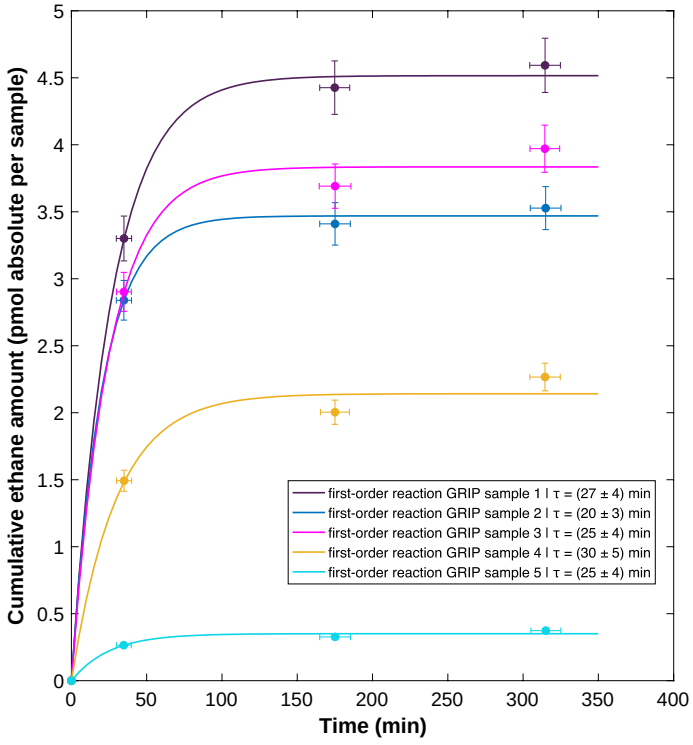

Figure B1: Temporal dynamics of excess ethane production in GRIP ice core samples. Cumulative ethane amount from the 1st, 2nd, and 3rd extraction in relation to the time available for a potential reaction in the melt water during each extraction. We assume a first-order reaction kinetic as model for our observations where the mean half-life time (τ) and standard deviations are calculated for each GRIP sample from the compilation of all 1000 iterations of our Monte Carlo approach assuming an uncertainty in x of ± 5 min and an uncertainty in y of ± 5 % of the measured value in the 1st extraction and ± 10 % in both the 2nd and 3rd extraction.

https://doi.org/10.5194/egusphere-2022-1133
Preprint. Discussion started: 10 November 2022

Author contribution

MM and BS performed the measurements; MM and JS analyzed the data; MM wrote the manuscript draft; MM prepared the manuscript with contributions from all co-authors.

Competing interests

The authors declare that they have no conflict of interest.

Acknowledgments

The research leading to these results has received funding from the Swiss National Science Foundation (no. 200020_172506 & 200020B_200328). This work is a contribution to the NorthGRIP ice core project, which is directed and organized by the Department of Geophysics at the Niels Bohr Institute for Astronomy, Physics and Geophysics, University of Copenhagen. It is supported by funding agencies in Denmark (SNF), Belgium (FNRS-CFB), France (IFRTP and NSU/CNRS), Germany (AWI), Iceland (RannIs), Japan (MEXT), Sweden (SPRS), Switzerland (SNF), and the United States (NSF).

https://doi.org/10.5194/egusphere-2022-1133
Preprint. Discussion started: 10 November 2022

References

Althoff, F., Jugold, A. and Keppler, F.: Methane formation by oxidation of ascorbic acid using iron minerals and hydrogen peroxide. Chemosphere 80, 286–292, https://doi.org/10.1016/j.chemosphere.2010.04.004, 2010

Althoff, F., Benzing, K., Comba, P., McRoberts, C., Boyd, D. R., Greiner, S. and Keppler, F.: Abiotic methanogenesis from organosulphur compounds under ambient conditions, Nat Commun, 5, 4205, https://doi.org/10.1038/ncomms5205, 2014

Anklin, M., Barnola, J.-M., Schwander, J., Stauffer, B., and Raynaud, D.: Processes affecting the CO_2 concentrations measured in Greenland ice, Tellus, 47, 461-470, https://doi.org/10.1034/j.1600-0889.47.issue4.6.x, 1995

Apel, K. and Hirt, H.: Reactive Oxygen Species: Metabolism, Oxidative Stress, and Signal Transduction, Annual Review of Plant Biology 2004, 55:1, 373-399, https://doi.org/10.1146/annurev.arplant.55.031903.141701, 2004

Austin, A. T., Méndez, M. S., and Ballaré, C. L.: Photodegradation alleviates the lignin bottleneck for carbon turnover in terrestrial ecosystems, PNAS, 13 (16), 4392-4397, https://doi.org/10.1073/pnas.1516157113, 2016

Baumgartner, M., Schilt, A., Eicher, O., Schmitt, J., Schwander, J., Spahni, R., Fischer, H., and Stocker, T. F.: High-resolution interpolar difference of atmospheric methane around the Last Glacial Maximum, Biogeosciences, 9, 3961–3977, https://doi.org/10.5194/bg-9-3961-2012, 2012

Baumgartner, M., Kindler, P., Eicher, O., Floch, G., Schilt, A., Schwander, J., Spahni, R., Capron, E., Chappellaz, J., Leuenberger, M., Fischer, H., and Stocker, T. F.: NGRIP CH_4 concentration from 120 to 10 kyr before present and its relation to a $\delta^{15}N$ temperature reconstruction from the same ice core, Clim. Past, 10, 903–920, https://doi.org/10.5194/cp-10-903-2014, 2014

Beck, J., Bock, M., Schmitt, J., Seth, B., Blunier, T., and Fischer, H.: Bipolar carbon and hydrogen isotope constraints on the Holocene methane budget, Biogeosciences, 15, 7155–7175, https://doi.org/10.5194/bg-15-7155-2018, 2018

Bernard, B., Brooks, J.M. and Sackett, W.M.: A geochemical model for characterization of hydrocarbon gas sources in marine sediments. In: 9th Annual Offshore Technology Conference, Houston, Texas, May 1977, 435–438 (OTC 2934), https://doi.org/10.4043/2934-MS, 1977

Bock, M., Schmitt, J., Behrens, M., Möller, L., Schneider, R., Sapart, C. and Fischer, H.: A gas chromatography/pyrolysis/isotope ratio mass spectrometry system for high- precision dD measurements of atmospheric methane extracted from ice cores, Rapid Commun. Mass Spectrom, 24, 621–633, https://doi.org/10.1002/rcm.4429, 2010a

Bock, M., Schmitt, J., Blunier, T., Fischer, H., Möller, L. and Spahni, R.: Hydrogen Isotopes Preclude Marine Hydrate CH4 Emissions at the Onset of Dansgaard- Oeschger Events, Science, 328, 1686-1689, https://doi.org/10.1126/science.1187651, 2010b

https://doi.org/10.5194/egusphere-2022-1133
Preprint. Discussion started: 10 November 2022

Bock, M., Schmitt, J., Beck, J., Schneider, R., and Fischer, H.: Improving accuracy and precision of ice core δD(CH_4) analyses using methane pre-pyrolysis and hydrogen post-pyrolysis trapping and subsequent chromatographic separation, Atmos. Meas. Tech., 7, 1999–2012, https://doi.org/10.5194/amt-7-1999-2014, 2014

Bock, M., Schmitt, J., Beck, J., Seth, B., Chappellaz, J. and Fischer, H.: Glacial/ interglacial wetland, biomass burning, and geologic methane emissions constrained by dual stable isotopic CH4 ice core records, PNAS, 114 (29), E5778-E5786, https://doi.org/10.1073/pnas.1613883114, 2017

Bory, A. J. M., Biscaye, P. E. and Grousset, F. E.: Two distinct seasonal Asian source regions for mineral dust deposited in Greenland (NorthGRIP), Geophys. Res. Lett. 30, 1167, https://doi.org/10.1029/2002GL016446, 2003

Biscaye P., Grousset F., Revel M., Van der Gaast S., Zielinski G., Vaars A. and Kukla, G.: Asian provenance of glacial dust (Stage 2) in the Greenland Ice Sheet Project 2 ice core, Summit, Greenland. J. Geophys. Res.-Oceans 102, 26765–26781, https://doi.org/10.1029/97JC01249, 1997

Bruhn, D., Mikkelsen, T. N., Øbro, J., Willats, W. G. T. and Ambus, P.: Effects of temperature, ultraviolet radiation and pectin methyl esterase on aerobic methane release from plant material, Plant Biology, 11, 43-48, https://doi.org/10.1111/j.1438-8677.2009.00202.x, 2009

Campen, R. K., Sowers, T., and Alley, R. B.: Evidence of microbial consortia metabolizing within a low-latitude mountain glacier, Geology, 31, 231–234, https://doi.org/10.1130/0091-7613(2003)031<0231:EOMCMW>2.0.CO;2, 2003

Chappellaz, J., Blunier, T., Kints, S., Dällenbach, A., Barnola, J. M., Schwander, J., Raynaud, D. and Stauffer B.: Changes in the atmospheric CH4 gradient between Greenland and Antarctica during the Holocene, Geophys. Res. Let., Volume 102, 15987-15997, https://doi.org/10.1029/97JD01017,1997

Cheng, A. L. and Huang, W. L.: Selective adsorption of hydrocarbon gases on clays and organic matter, Org. Geochem., 35, 413-423, https://doi.org/10.1016/j.orggeochem.2004.01.007, 2004

Dan, J., Kumai, T., Sugimoto, A. and Murase, J.: Biotic and abiotic methane releases from Lake Biwa sediment slurry, Limnology 5, 149–154, https://doi.org/10.1007/s10201-004-0124-7, 2004

Derendorp, L., Holzinger, R., Wishkerman, A., Keppler, F., and Röckmann, T.: VOC emissions from dry leaf litter and their dependence on temperature, Biogeosciences Discuss., 7, 823–854, https://doi.org/10.5194/bgd-7-823-2010, 2010

Derendorp, L., Holzinger, R., Wishkerman, A., Keppler, F., and Röckmann, T.: Methyl chloride and C2-C5 hydrocarbon emissions from dry leaf litter and their dependence on temperature, Atmospheric Environment, 45, 3112-3119, https://doi.org/10.1016/j.atmosenv.2011.03.016, 2011

https://doi.org/10.5194/egusphere-2022-1133
Preprint. Discussion started: 10 November 2022

Dumelin, E.E. and Tappel, A.L.: Hydrocarbon gases produced during in vitro peroxidation of polyunsaturated fatty acids and decomposition of preformed hydroperoxides, Lipids, 12, 894, https://doi.org/10.1007/BF02533308, 1977

Dyonisius, M. N., Petrenko, V. V., Smith, A.M., Hua, Q., Yang, B., Schmitt, J., Beck, J., Seth, B., Bock, M., Hmiel, B., Vimont, I., Menking, J. A., Shackleton, S. A., Baggenstos, D., Bauska, T. K., Rhodes, R., Sperlich, P., Beaudette, R., Harth, C., Kalk, M., Brook, E. J., Fischer, H., Severinghaus, J. P. and Weiss, R. F.: Old carbon reservoirs were not important in the deglacial methane budget, Science, 367(6480), 907-910, https://doi.org/10.1126/science.aax0504, 2020

Erhardt, T., Bigler, M., Federer, U., Gfeller, G., Leuenberger, D., Stowasser, O., Röthlisberger, R., Schüpbach, S., Ruth, U., Twarloh, B., Wegner, A., Goto-Azuma, K., Kuramoto, T., Kjær, H. A., Vallelonga, P. T., Siggaard-Andersen, M.-L., Hansson, M. E., Benton, A. K., Fleet, L. G., Mulvaney, R., Thomas, E. R., Abram, N., Stocker, T. F., and Fischer, H.: High resolution aerosol concentration data from the Greenland NorthGRIP and NEEM deep ice cores, Earth Syst. Sci. Data Discuss., 14, 1215–1231, https://doi.org/10.5194/essd-14-1215, 2022

Etiope, G. and Klusman, R. W.: Geologic emissions of methane to the atmosphere, Chemosphere, 49, 8, 777-789, https://doi.org/10.1016/S0045-6535(02)00380-6, 2002

Etiope G., Martinelli G., Caracausi, A. and Italiano, F.: Methane seeps and mud volcanoes in Italy: gas origin, fractionation and emission to the atmosphere, Geophys. Res. Lett., 34, https://doi.org/10.1029/2007GL030341, 2007

Etiope G., Lassey K. R., Klusman R. W. and Boschi, E.: Reappraisal of the fossil methane budget and related emission from geologic sources, Geophys. Res. Lett., 35, https://doi.org/10.1029/2008GL033623, 2008

Frahry, G. and Schopfer, P.: Hydrogen peroxide production by roots and its stimulation by exogenous NADH, Physiologia Plantarum, 103, 395-404, https://doi.org/10.1034/j.1399-3054.1998.1030313.x, 1998

Flückiger J., Blunier T., Stauffer B., Chappellaz M., Spahni R., Kawamura K., Schwander J., Stocker T. F. and Dahl-Jensen D.: N2O and CH4 variations during the last glacial epoch: Insight into global processes, Global Biogeochem. Cy 18, 1020, https://doi.org/10.1029/2003GB002122, 2004

Fuhrer, K. and Legrand, M.: Continental biogenic species in the Greenland Ice Core Project ice core: Tracing back the biomass history of the North American continent, J. Geophys. Res., 102(C12), 26735– 26745, https://doi.org/10.1029/97JC01299, 1997

Georgiou, C. D., Sun, H. J., McKay, C. P., Grintzalis, K., Papapostolou, I., Zisimopoulos, D., Panagiotidis, K., Zhang, G., Koutsopoulou, E., Christidis, G. E. and Margiolaki, I.: Evidence for photochemical production of reactive oxygen species in desert soils, Nat. Commun., 6, 7100, https://doi.org/10.1038/ncomms8100, 2015

Giorio, C., Kehrwald, N., Barbante, C., Kalberer, M., King, A. C. F., Thomas, E. R., Wolff, E. W. and Zennaro, P.: Prospects for reconstructing paleoenvironmental conditions from

https://doi.org/10.5194/egusphere-2022-1133
Preprint. Discussion started: 10 November 2022

organic compounds in polar snow and ice, Quaternary Science Reviews, 183, 1-22, https://doi.org/10.1016/j.quascirev.2018.01.007, 2018

Gu, Q., Chang, S. X., Wang, Z. P., Feng, J. C., Chen, Q. S. and Han, X. G.: Microbial versus non-microbial methane releases from fresh soils at different temperatures, Geoderma, 284, 178-184, https://doi.org/10.1016/j.geoderma.2016.08.027, 2016

Han, C., Do Hur, S., Han, Y., Lee, K., Hong, S., Erhard, T., Fischer, H., Svensson, A. M., Steffensen, J. P. and Vallelonga, P.: High-resolution isotopic evidence for a potential Saharan provenance of Greenland glacial dust. Sci Rep 8, 15582, https://doi.org/10.1038/s41598-018-33859-0, 2018

Helmig, D., Petrenko, V., Martinerie, P., Witrant, E., Röckmann, T., Zuiderweg, A., Holzinger, R., Hueber, J., Thompson, C., White, J. W. C., Sturges, W., Baker, A., Blunier, T., Etheridge, D., Rubino, M., and Tans, P.: Reconstruction of Northern Hemisphere 1950–2010 atmospheric non-methane hydrocarbons, Atmos. Chem. Phys., 14, 1463-1483, https://doi.org/10.5194/acp-14-1463, 2014

Hurkuck, M., Althoff, F., Jungkunst, H. F., Jugold, A. and Keppler, F.: Release of methane from aerobic soil: An indication of a novel chemical natural process?, Chemosphere, 86, 684-689, https://doi.org/10.1016/j.chemosphere.2011.11.024, 2012

Iseli, R.: Stable Isotope Analysis of Hydrogen in Methane using Antarctic Ice Cores. M.S. thesis, Climate and Environmental Physics, University of Bern, Switzerland, 2019

Ji L., Zhang T., Milliken K. L., Qu J. and Zhang X.: Experimental investigation of main controls to methane adsorption in clay-rich rocks, Appl. Geochem. 27, 2533–2545, https://doi.org/10.1016/j.apgeochem.2012.08.027, 2012

John, W. W. and Curtis, R. W.: Isolation and Identification of the Precursor of Ethane in Phaseolus vulgaris L., Plant Physiology, 59, 521–522, https://doi.org/10.1104/pp.59.3.521, 1977

Jugold, A., Althoff, F., Hurkuck, M., Greule, M., Lenhart, K., Lelieveld, J., and Keppler, F.: Non-microbial methane formation in oxic soils, Biogeosciences, 9, 5291–5301, https://doi.org/10.5194/bg-9-5291-2012, 2012

Katagi, T.: Photoinduced Oxidation of the organophosphorus Fungicide Tolclofs-methyl on Clay Minerals, J. Agrie. Food Cham., 38, 1595-1600, 1990

Kaufmann, P. R., Federer, U., Hutterli, M. A., Bigler, M., Schüpbach, S., Ruth, U., Schmitt, J. and Stocker, T. F.: An Improved Continuous Flow Analysis System for High-Resolution Field Measurements on Ice Cores, Environmental Science & Technology, 42 (21), 8044-8050, https://doi.org/10.1021/es8007722, 2008

Keeling, C. D.: The concentration and isotopic abundance of carbon dioxide in rural areas, Geochim. Cosmochim. Acta, 13, 322–334 https://doi.org/10.1016/0016-7037(58)90033-4.1958, 1958

https://doi.org/10.5194/egusphere-2022-1133
Preprint. Discussion started: 10 November 2022

Keeling, C. D.: The concentration and isotopic abundance of carbon dioxide in rural and marine air, Geochim. Cosmochim. Acta, 24, 277–298, https://doi.org/10.1016/0016-7037(61)90023-0, 1961

Keppler, F., Hamilton, J. T. G., Braß, M. and Röckmann, T.: Methane emissions from terrestrial plants under aerobic conditions, Nature 439, 187–191, https://doi.org/10.1038/nature04420, 2006

Keppler, F., Hamilton, J. T. G., McRoberts, W. C., Vigano, I., Braß, M. and Röckmann, T.: Methoxyl groups of plant pectin as a precursor of atmospheric methane: evidence from deuterium labelling studies, New Phytologist, 178, 808-814, https://doi.org/10.1111/j.1469-8137.2008.02411.x, 2008

Kibanova, D., Trejo, M., Destaillats, H. and Cervini-Silva, J.: Photocatalytic activity of kaolinite, Catalysis Communications, 12, 698-702, https://doi.org/10.1016/j.catcom.2010.10.029, 2011

Köhler, P., Fischer, H., Schmitt, J., and Munhoven, G.: On the application and interpretation of Keeling plots in paleo climate research – deciphering $\delta^{13}C$ of atmospheric CO_2 measured in ice cores, Biogeosciences, 3, 539–556, https://doi.org/10.5194/bg-3-539-2006, 2006

Lee, L. E., Edwards, J. S., Schmitt, J., Fischer, H., Bock, M. and Brook, E. J.: Excess methane in Greenland ice cores associated with high dust concentrations, Geochim. Cosmochim. Acta, 270, 409-430, https://doi.org/10.1016/j.gca.2019.11.020, 2020

Legrand, M., and Delmas, R.: Soluble Impurities in Four Antarctic Ice Cores Over the Last 30000 Years, Annals of Glaciology, 10, 116-120, https://doi.org/10.3189/S0260305500004274, 1988

Liu, J., Chen, H., Zhu, Q., Shen, Y., Wang, X., Wang, M., Peng, C.: A novel pathway of direct methane production and emission by eukaryotes including plants, animals and fungi: An overview, Atmospheric Environment, 115, 26, https://doi.org/10.1016/j.atmosenv.2015.05.019, 2015

Liu, D., Yuan, P., Liu, H., Li, T., Tan, D., Yuan, W., He, H.: High-pressure adsorption of methane on montmorillonite, kaolinite and illite, Applied Clay Science,85, 25-30, https://doi.org/10.1016/j.clay.2013.09.009, 2013

Lupker, M., Aciego, S. M., Bourdon, B., Schwander, J., and Stocker, T. F.: Isotopic tracing (Sr, Nd, U and Hf) of continental and marine aerosols in an 18th century section of the Dye-3 ice core (Greenland), Earth Pla Sci Let, 295, 277-286, https://doi.org/10.1016/j.epsl.2010.04.010, 2010

McLeod, A. R., Newsham, K. K. and Fry, S.C.: Elevated UV-B radiation modifies the extractability of carbohydrates from leaf litter of Quercus robur, Soil Biology and Biochemistry, 39, Issue 1, 116-126, https://doi.org/10.1016/j.soilbio.2006.06.019, 2007

McLeod, A.R., Fry, S.C., Loake, G.J., Messenger, D.J., Reay, D.S., Smith, K.A. and Yun, B.-W.: Ultraviolet radiation drives methane emissions from terrestrial plant pectins, New Phytologist, 180, 124-132, https://doi.org/10.1111/j.1469-8137.2008.02571.x, 2008

https://doi.org/10.5194/egusphere-2022-1133
Preprint. Discussion started: 10 November 2022

Messenger, D.J., McLeod, A. R. and Fry, S.C.: The role of ultraviolet radiation, photosensitizers, reactive oxygen species and ester groups in mechanisms of methane formation from pectin, Plant, Cell & Environment, 32: 1-9, https://doi.org/10.1111/j.1365-3040.2008.01892.x, 2009

Milkov, A. V. and Etiope, G.: Revised genetic diagrams for natural gases based on a global dataset of >20,000 samples, Organic Geochemistry, 125, 109-120, https://doi.org/10.1016/j.orggeochem.2018.09.002, 2018

Mitchell, L., Brook, E., Lee, J. E., Buizert, C., and Sowers, T.: Constraints on the Late Holocene anthropogenic contribution to the atmospheric methane budget, Science 342, 964–966, https://doi.org/10.1126/science.1238920, 2013

Miteva V., Teacher C., Sowers T. and Brenchley, J.: Comparison of the microbial diversity at different depths of the GISP2 Greenland ice core in relationship to deposition climates, Environ. Microbiol., 11, 640–656, https://doi.org/10.1111/j.1462-2920.2008.01835.x, 2009

Möller, L., Sowers, T., Bock, M., Spahni, R., Behrens, M., Schmitt, J., Miller, H. and Fischer, H.: Independent variations of CH4 emissions and isotopic composition over the past 160,000 years, Nature Geosci, 6, 885–890, https://doi.org/10.1038/ngeo1922, 2013

Mohnen, D.: Pectin structure and biosynthesis, Current Opinion in Plant Biology, 11, 266-277, https://doi.org/10.1016/j.pbi.2008.03.006, 2008

NEEM community members: Eemian interglacial reconstructed from a Greenland folded ice core, Nature, 493, 489–494, https://doi.org/10.1038/nature11789, 2013

Nicewonger, M. R., Verhulst, K. R., Aydin, M. and Saltzman, E. S.: Preindustrial atmospheric ethane levels inferred from polar ice cores: A constraint on the geologic sources of atmospheric ethane and methane, Geophys. Res. Lett., 43, https://doi.org/10.1002/2015GL066854, 2016

North Greenland Ice Core Project members, High-resolution record of Northern Hemisphere climate extending into the last interglacial period, *Nature* 431, 147–151, https://doi.org/10.1038/nature02805, 2004

Pires, J., Bestilleiro, M., Pinto, M. and Gil, A.: Selective adsorption of carbon dioxide, methane and ethane by porous clays heterostructures, Separation and Purification Technology, 61, 161-167, https://doi.org/10.1016/j.seppur.2007.10.007, 2008

Price, P. B. and Sowers, T.: Temperature dependence of metabolic rates for microbial growth, maintenance, and survival, P. Natl. Acad. Sci. USA 101, 4631–4636, https://doi.org/10.1073/pnas.0400522101, 2004

Rohde, R. A., Price, P. B., Bay, R. C. and Bramall, N. E.: In situ microbial metabolism as a cause of gas anomalies in ice, P. Natl. Acad. Sci. USA, 105, 8667–8672, https://doi.org/10.1073/pnas.0803763105, 2008

https://doi.org/10.5194/egusphere-2022-1133
Preprint. Discussion started: 10 November 2022

Rhodes, R. H., Faïn, X., Stowasser, C., Blunier, T., Chappellaz, C., McConnell, J. R., Romanini, D., Mitchell, L. E. and Brook, E. J.: Continuous methane measurements from a late Holocene Greenland ice core: Atmospheric and in situ signals, Earth and Planetary Science Letters, 368, 9-19, https://doi.org/10.1016/j.epsl.2013.02.034, 2013

Rhodes, R. H., Faïn, X., Brook, E. J., McConnell, J. R., Maselli, O. J., Sigl, M., Edwards, J., Buizert, C., Blunier, T., Chappellaz, J., and Freitag, J.: Local artifacts in ice core methane records caused by layered bubble trapping and in situ production: a multi-site investigation, Clim. Past, 12, 1061–1077, https://doi.org/10.5194/cp-12-1061-2016, 2016

Ross, D. J. K. and Bustin, R. M.: The importance of shale composition and pore structure upon gas storage potential of shale gas reservoirs, Mar. Petrol. Geol., 26, 916-927, https://doi.org/10.1016/j.marpetgeo.2008.06.004, 2009

Ruth, U., Wagenbach, D., Steffensen, J. P. and Bigler, M.: Continuous record of microparticle concentration and size distribution in the central Greenland NGRIP ice core during the last glacial period, J. Geophys. Res., 108 (D3), 4098, https://doi.org/10.1029/2002JD002376, 2003

Schade, G. W., Hofmann, R.-M. and Crutzen, P. J.: CO emissions from degrading plant matter, Tellus B: Chemical and Physical Meteorology, 51:5, 889-908, https://doi.org/10.3402/tellusb.v51i5.16501, 1999

Schilt, A., Baumgartner, M., Blunier, T., Schwander, J., Spahni, R., Fischer, H., and Stocker, T. F.: Glacial–interglacial and millennial-scale variations in the atmospheric nitrous oxide concentration during the last 800,000 years, Quat Sci Rev, 29, 182-192, https://doi.org/10.1016/j.quascirev.2009.03.011, 2010

Schmitt, J., Seth, B., Bock, M. and Fischer, H.: Online technique for isotope and mixing ratios of CH4, N2O, Xe and mixing ratios of organic trace gases on a single ice core sample, Atmos. Meas. Tech., 7, 2645–2665, https://doi.org/10.5194/amt-7-2645-2014, 2014

Smith, H. J., Wahlen, M., Mastroianni, D., and Taylor, K. C.: The CO_2 concentration of air trapped in GISP2 ice from the Last Glacial Maximum-Holocene transition, Geophys Res Let, 24, 1-4, https://doi.org/10.1029/96GL03700, 1997

Sugimoto, A., Dan, J., Kumai, T. and Murase J.: Adsorption as a methane storage process in natural lake sediment, Geophys. Res. Lett. 30, 2080, https://doi.org/10.1029/2003GL018162, 2003

Svensson, A., Biscaye, P. E. and Grousset, F. E.: Characterization of late glacial continental dust in the Greenland Ice Core Project ice core, J. Geophys. Res.-Atmos., 105, 4637–4656, https://doi.org/10.1029/1999JD901093, 2000

Tian, Y., Yan, C. and Jin, Z.: Characterization of Methane Excess and Absolute Adsorption in Various Clay Nanopores from Molecular Simulation, Sci Rep 7, 12040, https://doi.org/10.1038/s41598-017-12123, 2017

Tung, H. C., Bramall, N. E. and Price, P. B.: Microbial origin of excess methane in glacial ice and implications for life on Mars, P. Natl. Acad. Sci. USA 102, 18292–18296, https://doi.org/10.1073/pnas.0507601102, 2005

https://doi.org/10.5194/egusphere-2022-1133
Preprint. Discussion started: 10 November 2022

Tung, H., Price, P., Bramall, N. and Vrdoljak G.: Microorganisms metabolizing on clay grains in 3-km-deep Greenland basal ice, Astrobiology 6, 69–86. https://doi.org/10.1089/ast.2006.6.69, 2006

Vigano, I., van Weelden, H., Holzinger, R., Keppler, F., McLeod, A., and Röckmann, T.: Effect of UV radiation and temperature on the emission of methane from plant biomass and structural components, Biogeosciences, 5, 937–947, https://doi.org/10.5194/bg-5-937-2008, 2008

Vigano, I., Röckmann, T., Holzinger, R., van Dijk, A., Keppler, F., Greule, M., Brand, W. A., Geilmann, H. and van Weelden, H.: The stable isotope signature of methane emitted from plant material under UV irradiation, Atmospheric Environment, 43, 5637-5646, https://doi.org/10.1016/j.atmosenv.2009.07.046, 2009

Vigano, I., Holzinger, R., Keppler, F., Greule, M., Brand, W. A., Geilmann, H., van Weelden, H. and Röckmann,T.: Water drives the deuterium content of the methane emitted from plants, Geochimica et Cosmochimica Acta,74, 3865-3873, https://doi.org/10.1016/j.gca.2010.03.030, 2010

Wang, Z.P., Han, X.G., Wang, G.G., Song, Y. and Gulledge, J.: Aerobic methane emission from plants in the Inner Mongolia steppe, Environmental Science & Technology 42, 62– 68 https://doi.org/10.1021/es071224l, 2008

Wang, Z.P., Xie, Z.Q., Zhang, B.C., Hou, L.Y., Zhou, Y.H., Li, L.H. and Han, X.G.: Aerobic and Anaerobic Nonmicrobial Methane Emissions from Plant Material, Environmental Science & Technology 2011 45 (22), 9531-9537, https://doi.org/10.1021/es2020132, 2011

Wang, B., Hou, L., Liu, W. and Wang, Z.: Non-microbial methane emissions from soils, Atmospheric Environment, 80, 290–298, https://doi.org/10.1016/j.atmosenv.2013.08.010, 2013

Wang, B., Lerdau, M. and He, Y.: Widespread production of nonmicrobial greenhouse gases in soils, Glob Change Biol., 23:4472–4482, https://doi.org/10.1111/gcb.13753, 2017

Watanabe, M., Watanabe, Y., Kim, Y. S., Koike, T.: Dark aerobic methane emission associated to leaf factors of two Acacia and five Eucalyptus species, Atmospheric Environment, 54, 277-281, https://doi.org/10.1016/j.atmosenv.2012.02.012, 2012

Whiticar, M. J.: Carbon and hydrogen isotope systematics of bacterial formation and oxidation of methane, Chemical Geology, 161, 291-314, https://doi.org/10.1016/S0009-2541(99)00092-3, 1999

Wu, F., Li, J., Peng, Z., Deng, N.: Photochemical formation of hydroxyl radicals catalyzed by montmorillonite, Chemosphere, 72, 407-413, https://doi.org/10.1016/j.chemosphere.2008.02.034, 2008

York, D.: Least squares fitting of a straight line with correlated errors, Earth and Planetary Science Letters, 5, 320-324, https://doi.org/10.1016/S0012-821X(68)80059-7, 1968

York, D., Evensen, N. M., Martınez, M. L., and De Basabe Delgado, J.: Unified equations for the slope, intercept, and standard errors of the best straight line, Am. J. Phys. 72, 367–375, https://doi.org/10.1119/1.1632486, 2004